Geol. Mag. **144** (*3*), *2007, pp. 525–546. © 2007 Cambridge University Press*
doi:10.1017/S0016756807003299 First published online 30 March 2007 *Printed in the United Kingdom*

Mesoproterozoic dyke swarms in foreland and nappes of the central Scandinavian Caledonides: structure, magnetic fabric, and geochemistry

R. O. GREILING*†, J. C. GRIMMER*, H. DE WALL‡ & L. BJÖRK§

*Geologisch-Paläontologisches Institut, Ruprecht-Karls-Universität Heidelberg, Im Neuenheimer Feld 234, D-69120 Heidelberg, FRG
‡Geologisches Institut, Universität Würzburg, Pleicherwall 1, D-97070 Würzburg, FRG
§Sveriges Geologiska Undersökning, Box 670, S-75128 Uppsala, Sweden

(*Received* 30 December 2005; *accepted* 1 August 2006)

Abstracts – As an example of microstructural and magnetic fabric evolution, and geochemistry of mafic dykes during a subsequent orogenic overprint, a major Mesoproterozoic dyke complex in Scandinavia, the Västerbotten complex of the Central Scandinavian Dolerite Group, is traced westwards into the crystalline nappes of the early Phanerozoic Caledonian orogen. Using geophysical, field, microscopic, magnetic and geochemical information, dykes and sills are characterized, and their overprint during Caledonian orogeny documented. The Västerbotten complex is composed of sets of dykes, trending NE–SW, NW–SE and WNW–ESE, respectively. Similar dykes are exposed in allochthonous positions (Lower and Middle allochthons) in the Caledonian fold-and-thrust belt. The autochthonous dykes are generally undeformed and retain both their primary texture and mineralogy. Chilled margins are well preserved. In the Caledonian Lower and Middle allochthons, similar dykes in crystalline basement rocks are progressively faulted and sheared when proceeding from the marginal to the interior parts of the orogen. Dyke margins are more likely to be sheared than the interior parts of dykes. In the Lower Allochthon, under very low- and low-grade metamorphic conditions, dykes are distinctly less competent than granitic host rocks. Thick dykes are more competent than gneisses; thin dykes do not show such competence contrasts. In the Middle Allochthon, metre-scale dykes with patches of altered plagioclase phenocrysts can still be discerned in low-strain domains. Highly sheared dykes are drawn out to thin layers of centimetre thickness. Dykes are deformed together with the crystalline country rocks under greenschist-grade metamorphic conditions without major competence contrasts. Magnetic fabrics show an evolution similar to the silicate mineral fabrics. The magnetic fabrics in the dykes are transformed successively from ferromagnetic–magmatic in the Autochthon to ferromagnetic deformational in the Lower Allochthon and, finally, paramagnetic deformational in the Middle Allochthon. As a consequence, the magnetic susceptibility decreases for several orders of magnitude. Geochemically, the dykes are dominantly sub-alkaline basalts typical for continental tholeiites and can be distinguished from the Neoproterozoic dykes in the Särv-Nappe equivalents (highest part of the Middle Allochthon), which show a more MORB-like (E-MORB) magmatic signature. Preliminary age information from a dyke in the Lower Allochthon of the Børgefjell area and the Middle Allochthon is consistent with the assumption that these dykes are time equivalent with the Central Scandinavian Dolerite Group. Therefore, the studied dykes may represent an extension of the Västerbotten complex or a new complex of the Central Scandinavian Dolerite Group. According to section restorations, the Caledonian allochthons were situated further WNW relative to their present position, and, originally, the mafic dykes cut across all of the Fennoscandian lithosphere, at least to the present Atlantic margin and the earlier passive margin of the Baltica terrane. As a consequence, these dykes may provide a link for pre-Caledonian and pre-Grenvillian plate reconstructions.

Keywords: dykes, microstructure, magnetic anisotropy, geochemistry, dolerite, Caledonides, Scandinavia.

1. Introduction

Mafic dyke swarms are significant tectonic features of continental crust and have added substantial volumes to it, with major contributions in Proterozoic times (e.g. Tarney, 1992; Condie, 2003; Windley, 2003). These dyke swarms originate from melts created in the uppermost mantle and may, therefore, indicate ancient sites of melting above mantle plumes (Ernst & Buchan, 2001*a*). However, post-intrusive tectonic and sedimentary processes frequently obscure the dyke swarms, and many aspects of dyke formation, distribution and behaviour during subsequent tectonic overprint are not yet fully understood. As an example of such dykes,

† Author for correspondence: er8@ix.urz.uni-heidelberg.de

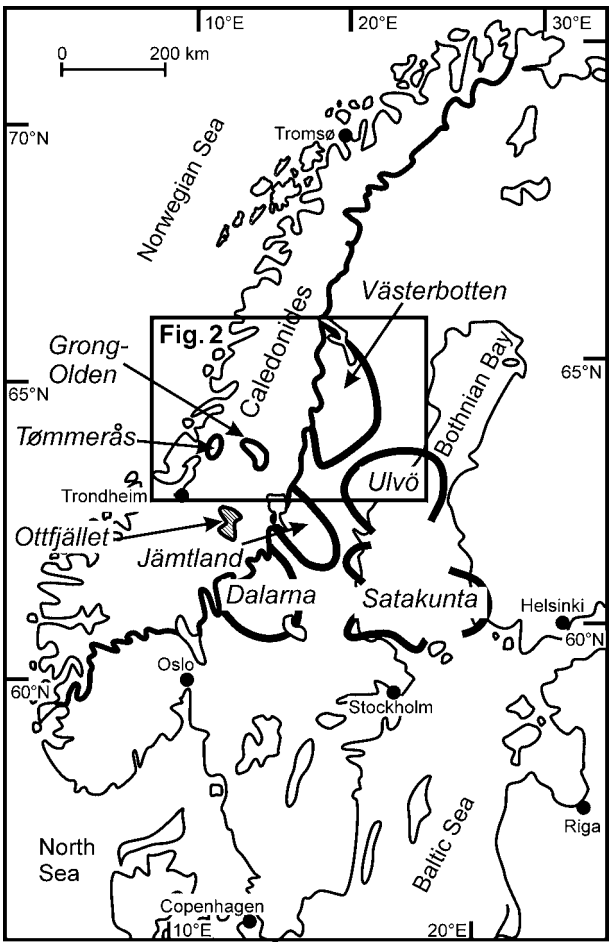

Figure 1. Outline of the western part of the Fennoscandian Shield with the dyke complexes (delimited by thick, black lines) that comprise the Central Scandinavian Dolerite Group as defined by Gorbatschev, Solyom & Johansson (1979) and modified by Hogmalm *et al.* (2006). The study area is shown in more detail on Figure 2, whose location is marked by a box. In addition, the locations of dykes in the Grong-Olden and Tømmerås areas of the Scandinavian Caledonides are indicated. The Ottfjället dykes are situated in a structurally higher unit, geochemically different, and are shown with a hatched pattern. Compiled from Johannsson (1980) and Koistinen *et al.* (2001).

this study focuses on a major Mesoproterozoic dyke complex in Scandinavia, the Västerbotten complex of the Central Scandinavian Dolerite Group (Fig. 1), and its westward continuation within the crystalline nappes of the early Phanerozoic Caledonian orogen. The incorporation into the Caledonian thrust units led to deformation and metamorphism so that the mafic dyke rocks can now be used as 'markers' for the Caledonian overprint and can be compared with their undeformed and unmetamorphic equivalents in the Fennoscandian Shield. Using geophysical, field, microscopic, magnetic and geochemical information, dykes and sills are characterized, and their overprint during Caledonian orogeny documented. Starting with a regional introduction, the distribution, fabric characteristics, strain, magnetic fabric and geochemistry are presented in successive chapters. A final discussion assesses the significance of the new data.

1.a. Regional context

A number of late Mesoproterozoic dyke swarms and sill complexes intruded the Fennoscandian Shield at *c.* 1265 Ma ago (Ernst & Buchan, 2001*b*; Söderlund *et al.* 2005; see Fig. 1). The major part of the shield had been a craton since the end of the Svecofennian orogeny in Palaeoproterozoic times (*c.* 1.8 Ga ago: Stephens, Wahlgren & Weihed, 1997; Lundqvist & Autio, 2000). It is broadly composed of an Archaean 'nucleus' in the north with a magmatic arc at its southern margin. This magmatic arc comprises the Skellefte area in northern Sweden and is bounded southwards by the oceanic Bothnian Basin. The southern margin of the Bothnian Basin is formed by another magmatic arc in central Sweden (e.g. Bergslagen). The rocks of the Bothnian Basin comprise major clastic greywacke sequences and subordinate early intrusives (gabbros, granitoids) and volcanic rocks. Late Svecofennian, *c.* 1.8 Ga old granitoids intruded the succession and are mostly undeformed. The western part of these terranes is partly overprinted by the intrusive suites of the broadly N–S-trending Transscandinavian Igneous Belt of late Palaeoproterozoic age (Lundqvist & Autio, 2000; Hellström & Larson, 2003; Högdahl, Andersson & Eklund, 2004). Towards the west, the Shield is overlain by a thin, discontinuous sedimentary cover of late Neoproterozoic to Ordovician age and the fold-and-thrust belt of the Caledonian orogen. The lower units within the latter represent the Fennoscandian passive continental margin (Lower Allochthon and lower part of the Middle Allochthon) and ocean–continent transition (upper part of Middle Allochthon–Särv Nappe, and lower part of Upper Allochthon–Seve Nappe) of late Neoproterozoic to early Palaeozoic age. The Särv Nappe is famous for its dyke swarms (e.g. Ottfjället dyke swarm; see Fig. 1), which are related to the continental break-up and early ocean opening in late Neoproterozoic times (Solyom, Gorbatschev & Johansson, 1979; Gilotti & Kumpulainen, 1986). However, these dykes are distinct from the dykes of the Fennoscandian Shield in their chemical composition and clearly younger age (late Neoproterozoic versus late Mesoproterozoic). Johansson (1980) documented mafic dykes and sills within the crystalline parts of the Lower Allochthon in the Grong-Olden Culmination (see Fig. 1). Subsequently, more occurrences of mafic dykes have been found in lower Caledonian units further north (G. Eberz, unpub. Diploma thesis, Mainz Univ., 1982; Greiling, 1982, 1985, 1988; Greiling *et al.* 1984). Since then, detailed mapping has provided comprehensive coverage of the area and revealed further mafic dykes in the Caledonian Lower and

https://doi.org/10.1017/S0016756807003299 Published online by Cambridge University Press

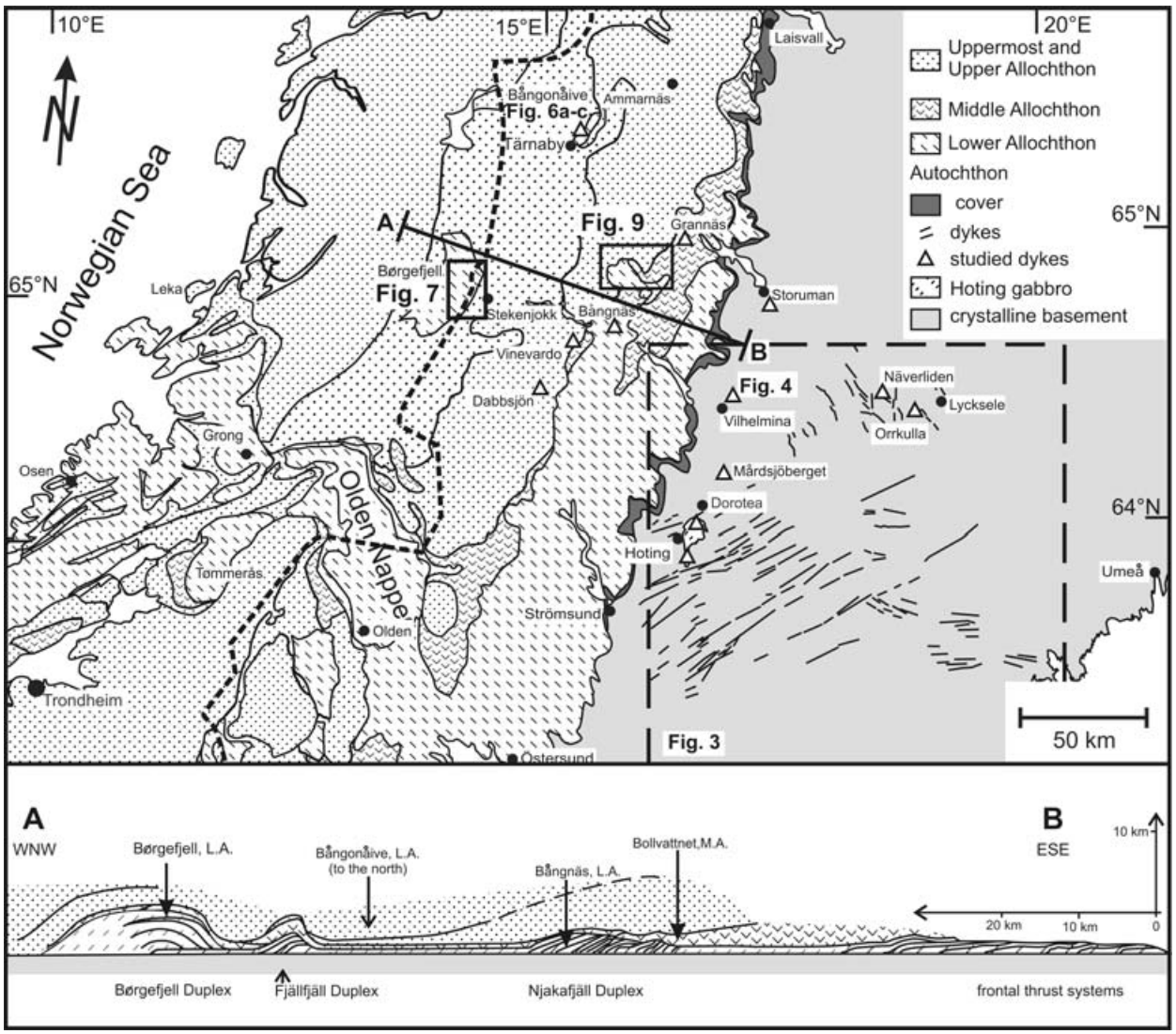

Figure 2. Major rock units in central Scandinavia, with the Västerbotten complex dykes in the Fennoscandian Shield. Detailed maps of dykes in the Caledonian nappes (Lower and Middle allochthons) are shown on Figures 7 and 9, respectively (location marked by boxes). Bottom: structural section across the Caledonian part of the study area, showing the thin-skinned character of the fold-and-thrust belt and the relative position of the studied dykes in the Lower and Middle allochthons (L. A., M. A., respectively). Location of section line is marked A–B on the map above; legend as for the map.

Middle allochthons (e.g. Zachrisson & Greiling, 1993; Greiling & Zachrisson, 1999).

1.b. The Västerbotten complex in the Central Scandinavian Dolerite Group

The Central Scandinavian Dolerite Group (Gorbatschev, Solyom & Johansson, 1979) in a strict sense covers an area delimited by the Caledonian margin in the west and the eastern coastal areas of the Bothnian Bay in the east. It is composed of a number of distinct dyke and sill complexes, which in themselves comprise several dyke and sill swarms (Fig. 1). Following the fundamental work of Gorbatschev, Solyom & Johansson (1979) in Jämtland, further complexes were found in the adjacent Fennoscandian Shield. The latest addition has been the northern Sweden or Västerbotten complex (Elming & Mattsson, 2001). It is composed of several sets of parallel dykes, as well as major sills and related intrusions. During the last decade, detailed mapping at the scale of 1:50 000, supported by magnetic anomaly maps, revealed the exact geometry and extent of a major part of this complex (Figs 2, 3; e.g. Björk, Kero & Zachrisson, 2000; Björk & Kero, 2002; Koistinen *et al.* 2001; Kathol & Weihed, 2005). Accordingly, the northern part of the Västerbotten complex is composed of several sets of dykes, trending NE–SW, NW–SE and WNW–ESE, respectively (Fig. 2). Based on different palaeomagnetic pole directions, Elming, Moakhar & Martinsson (2004) distinguished two generations of dykes.

https://doi.org/10.1017/S0016756807003299 Published online by Cambridge University Press

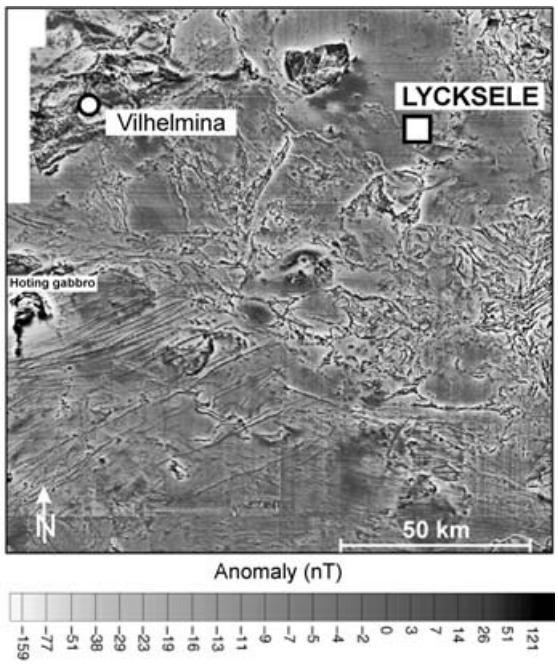

Figure 3. Magnetic anomaly map covering the autochthonous crystalline basement to the east of the Caledonian belt, shown in Figure 2. From the aeromagnetic database © Geological Survey of Sweden (SGU). Note clear images of NE–SW-trending dykes to the east and south of the Hoting gabbro. Some of these dykes can also be seen to cut across this gabbro. WNW–ESE-trending dykes show up in the lower central parts of the map. In the northern and eastern parts of the map, dykes contrast less clearly with the irregular stripes representing supracrustal sequences. Sub-circular anomaly patterns reflect the shape of intrusive bodies.

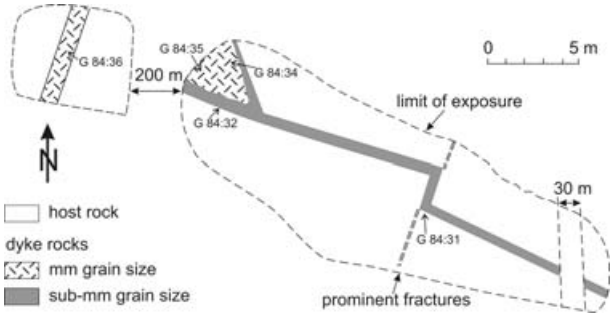

Figure 4. Map view of steeply dipping dykes in granite at Granberget, about 5 km east of Vilhelmina at the south side of the Vilhelmina–Lycksele road (see Björk, Kero & Zachrissson, 2000). The location of samples is indicated.

2. Examples of Västerbotten complex dykes in the autochthonous, crystalline basement

Mafic dykes contrast well with the dominantly granitoid Svecofennian country rocks of the Fennoscandian Shield, both with respect to lithology and to magnetic properties. Therefore, the large-scale geometry of the dyke swarms can be well determined from magnetic anomaly maps (Fig. 3). In the field, however, the complete geometry of individual dykes is not always accessible due to limited exposure. Dyke thicknesses range from less than 1 m to more than a hundred metres.

A typical example is exposed near Vilhelmina, along the road to Lycksele (Björk, Kero & Zachrisson, 2000). While the dyke in general is several metres thick, marginal parts are less than 1 m thick (Fig. 4). This difference in thickness is also reflected in the primary texture. The thinner parts of the dykes show a well-developed chilled margin. The micrographs of Figure 5 (a, b) show a sequence from the country rock–dyke contact across the chilled margin and towards the central part of the dyke. At the contact, the dyke has a sub-microscopic grain size for a width of about 5 mm. Towards the interior, millimetre-size phenocrysts of pyroxene and plagioclase come in, and further inwards, there is an increase in the matrix grain size from a few micrometres to several millimetres. The interior parts of the dykes are characterized by relatively coarse-grained, ophitic to intergranular intergrowths of pyroxene and plagioclase, with subordinate opaque minerals and olivine. Chilled margins can also be observed at the Mårdsjöberget dykes and those further south, which cut across the Hoting gabbro and its country rocks (Fig. 2). Relatively thick dykes and sills, for example, the several-metres-thick sill at Storuman (Stålhös, 1958), have a coarse-grained ophitic texture throughout (Fig. 5c, d) and no distinct chilled margin. The dykes at Näverliden also show a coarse ophitic texture, although the contacts with the country rock have not been observed.

Although the dykes in the Fennoscandian Shield are generally undeformed, several pre- and post-emplacement deformation features can be documented. At the Vilhelmina dyke, quartz of the country rock shows undulatory extinction (Fig. 5a). Plagioclase fragments with deformed twin lamellae are also found within the dyke close to the margin. However, these are unlike the observed plagioclase phenocrysts and were probably derived from the earlier deformed country rock and incorporated into the dyke during intrusion. In the dyke itself, minerals are undeformed. Therefore, deformation is apparently older than dyke intrusion. As is shown in Figure 4, a deformation zone in the country rock coincides with a bend in the dyke. Therefore, it is likely that the dyke exploited the pre-existing deformation zone during propagation as long as it was oriented favourably for melt intrusion. Bent and broken plagioclase phenocrysts can sometimes be observed within a fabric of undeformed, randomly oriented minerals (Fig. 5c, d). Apparently, such crystals were deformed at a late stage of dyke intrusion, when phenocrysts had already crystallized but the melt was still moving. Distinct post-emplacement deformation could be observed at a dyke south of the Hoting gabbro, which is cut by a (brittle) fault.

https://doi.org/10.1017/S0016756807003299 Published online by Cambridge University Press

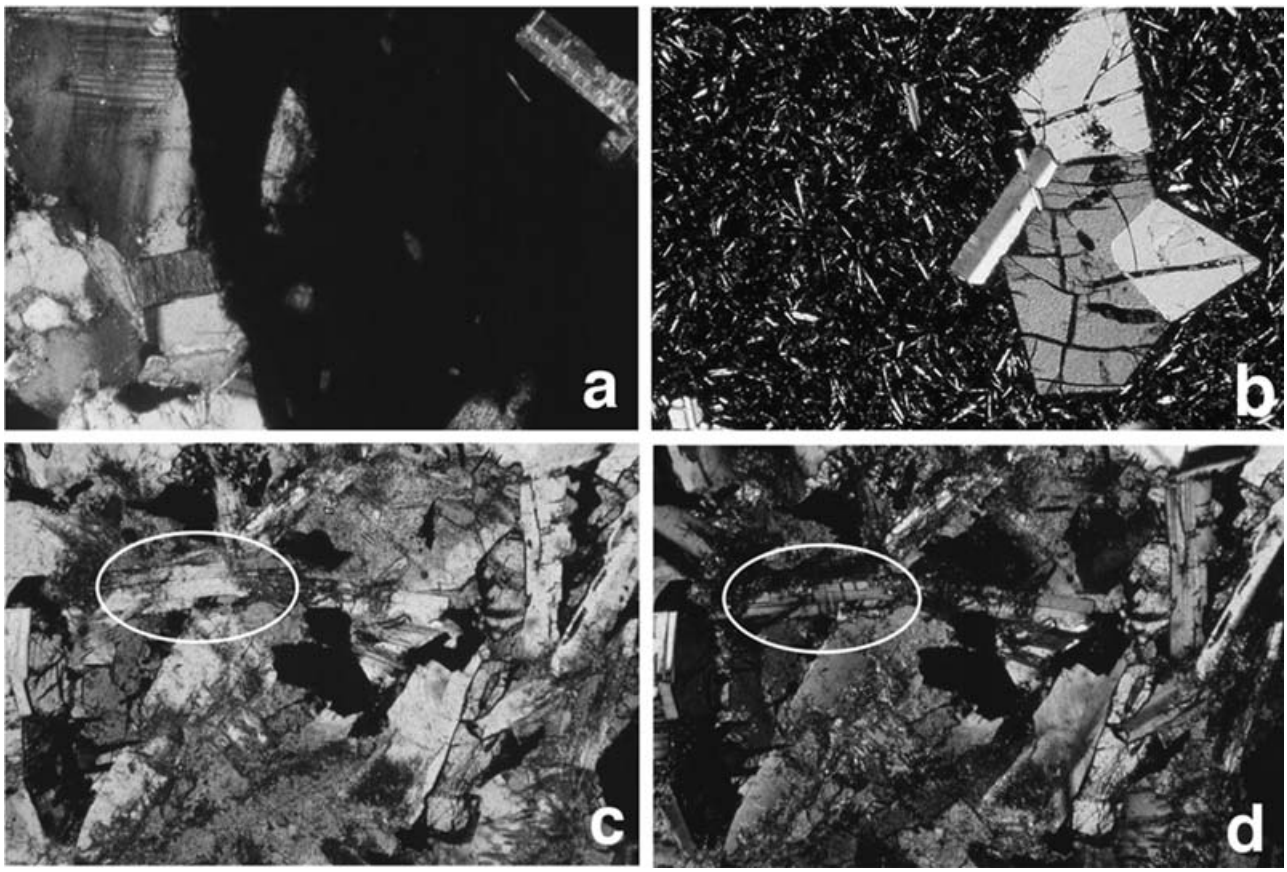

Figure 5. Micrographs of dykes in the Fennoscandian Shield. (a, b) Micrographs from a chilled margin of a dyke at Granberget, sample G84:31; see Figure 4. Horizontal margin corresponds to 2.3 mm in length. (a) Granitic host rock at left, very fine-grained dyke margin at right. Deformation twins in feldspar are related to pre-dyke fracture, and apparent 'phenocrysts' are probably derived from the host rock. (b) Increase in frequency and grain size of minor phenocrysts towards fine-grained ophitic texture from left to right, and aggregate of pyroxene phenocrysts. The latter are altered along cracks. (c, d) Coarse, ophitic texture, representing the general appearance of Västerbotten complex dykes. Sample G80155, location Storuman, see Figure 2. Horizontal margin is 2.3 mm in nature; (c) plane polarized light, (d) crossed polarizers. Pyroxene and opaque minerals fill the spaces between plagioclase laths. Note bent and broken plagioclase crystal, which shows deformation twins with crossed polarizers (ellipse).

3. Mafic dykes in the Lower and Middle allochthons of the Caledonian nappes

Mafic dykes are distributed exclusively within the crystalline parts of the Caledonian Lower Allochthon and the lower thrust units of the Middle Allochthon. No dykes have been observed in the sedimentary cover rocks. Therefore, the dykes can be assumed to be older than the cover rocks. An exception is the Särv Nappe (see Section 3.b.2).

3.a. Lower Allochthon

In the eastern, external part of the orogenic belt, deformation within the thrust units is moderate, and primary contact relationships are well preserved. Dykes can be seen to cut across the earlier crystalline rocks and their fabrics. These country rocks are mostly granitoid rocks, with minor bodies of mafic intrusions. Although generally well preserved and only weakly overprinted by deformation and very low-grade metamorphism, dykes in the Caledonian marginal part of the Lower Allochthon are often poorly exposed, due to Quaternary cover sediments. These accumulated (or were hardly removed) by glacial processes at the low-lying margin of the mountain belt, which also happened to be close to the former ice divide between the Atlantic Ocean and Baltic Sea. Therefore, only one sample is available from the Bångnäs dyke (see location on Fig. 2; also Zachrisson & Greiling, 1993).

Further west, towards the interior of the orogen, where the Lower Allochthon is exposed in tectonic windows, dykes are better accessible. In the Bångonåive window a mafic dyke is exposed which cuts across syenitic country rocks (Fig. 2; Greiling, 1982; Greiling, Gayer & Stephens, 1993). The dyke still retains its steep orientation and sharp contacts (Fig. 6a), although its fabric is more strongly overprinted than that of dykes in a more eastern, more external, position within the orogen. Figure 6 (b, c) shows remnants of an ophitic texture. Primary minerals are in a state of transformation into a secondary mineral assemblage, mainly

https://doi.org/10.1017/S0016756807003299 Published online by Cambridge University Press

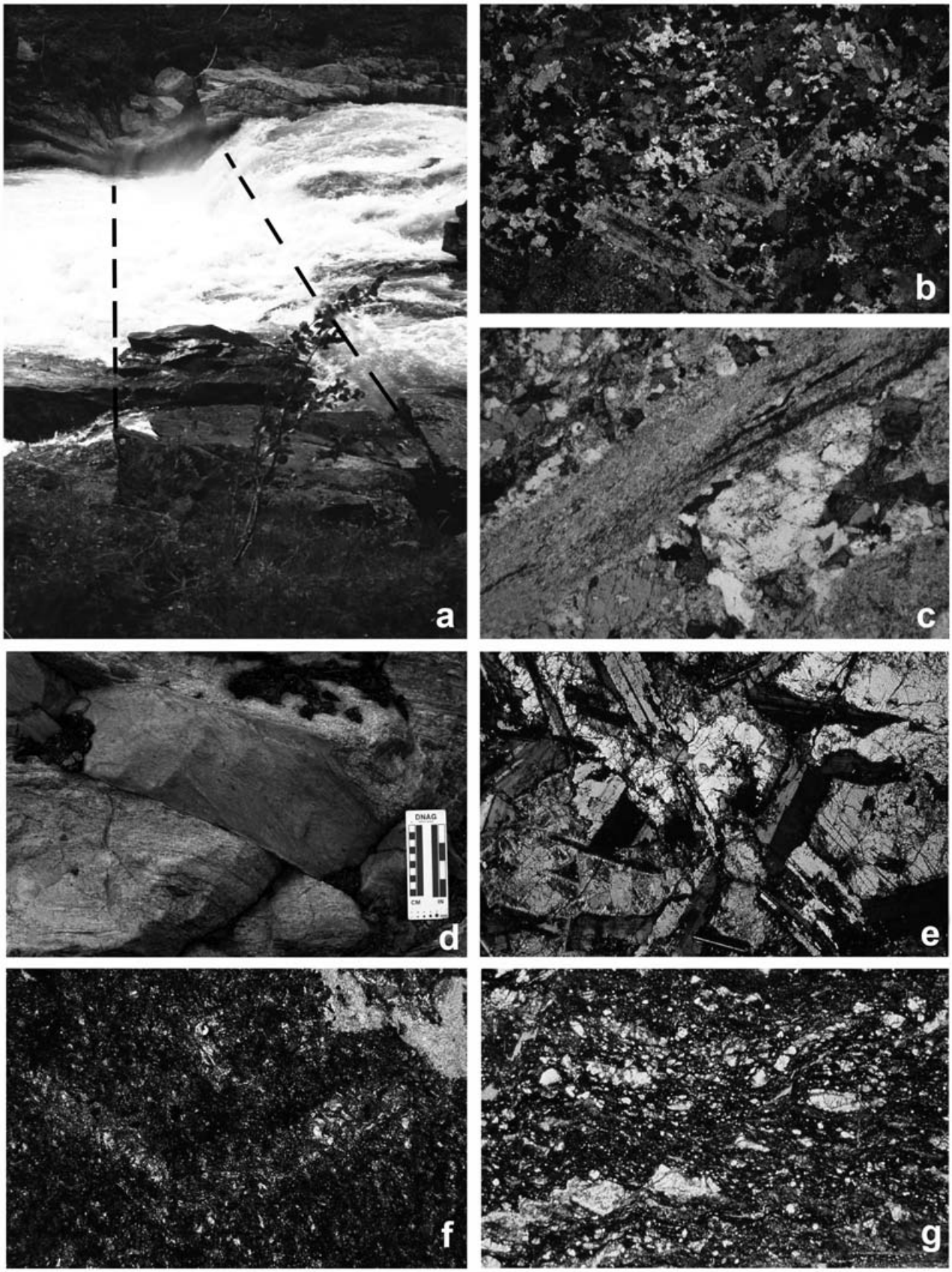

Figure 6. Field photographs and micrographs of dykes in the Lower Allochthon of (a–c) the Bångonåive Window and (d–g) the Børgefjell Window; see Figures 2, 7 and 8 for location. (a) Field view of mafic dyke in syenite host rock, looking west over Tärnaån stream. Small birch tree in foreground is about 1 m high. (b) Micrograph of dyke with relic ophitic texture in the lower part, defined by plagioclase laths. Plagioclase crystals are in the course of being replaced by sericite and calcite. The upper part is completely

https://doi.org/10.1017/S0016756807003299 Published online by Cambridge University Press

albite, biotite, calcite, sericite of lower greenschist metamorphic grade. This sample with relatively well-preserved remnants of primary textures is characteristic of the central parts of dykes. The margins of the dyke are more strongly sheared and there is no clear evidence of a primary texture preserved. Figure 6c shows a fine-grained albite–sericite aggregate, which appears to be pseudomorphous after a primary plagioclase phenocryst. This 'pseudomorph' represents an intermediate stage in a sequence of progressive deformation, which starts with well-preserved outlines of replaced plagioclase crystals and ends with a completely sheared state, when the former phenocryst pseudomorph is indistinguishable from the matrix. The aggregate of Figure 6c contains two sets of surfaces oriented at low angles with each other. Displacement of the older surfaces along the more prominent, younger surfaces is clear and implies that the fabric represents an S–C fabric.

In the westernmost parts of the Lower Allochthon, in the Børgefjell window (Fig. 7), both low-strain and relatively high-strain domains can be observed. It is not immediately obvious why some of the dykes are sheared, whereas others are not. One of the causes may simply be dyke thickness and related different grain sizes. While an approximately 30 m thick major dyke is hardly deformed (Fig. 6e), a thin 'offshoot' is intensely foliated (Figs 6d, 8). The major dyke itself displays features similar to the one from the Bångonåive window (above, Fig. 6a), with a little deformed and hardly altered central part (Fig. 6e). Mineral phase changes are restricted to the margins of the primary minerals (Fig. 6e). Figure 6f represents the dyke margin with albite, sericite, epidote, clinozoisite documenting a lower greenschist-grade metamorphic overprint. Other dykes of the Børgefjell window are both more strongly altered and more strongly foliated. Figure 6g gives an example of a foliated dyke rock, where albite and plagioclase grains are sheared into lenses, documenting a strong simple shear component of deformation. Such a simple shear deformation is likely to be related to thrusting and stacking of the Børgefjell duplex (e.g. Greiling, Garfunkel & Zachrisson, 1998).

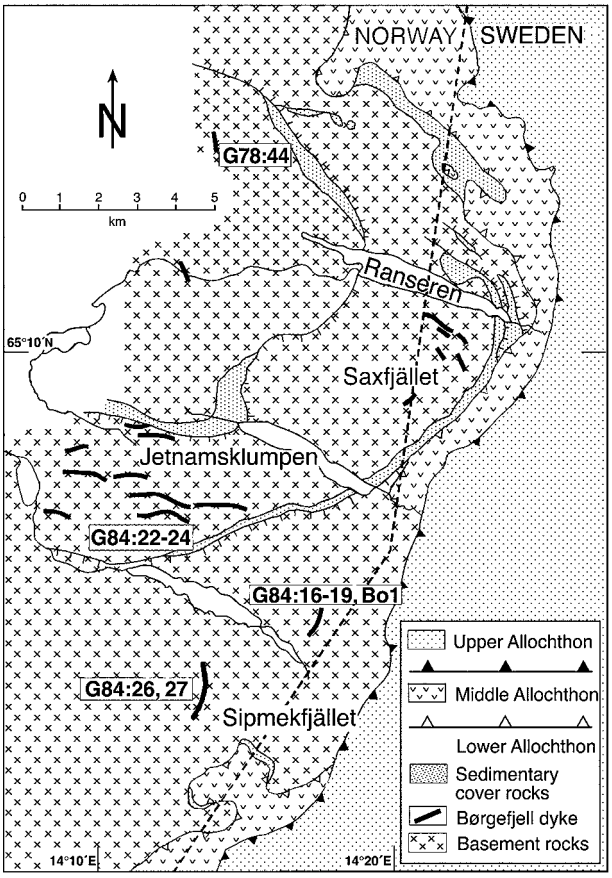

Figure 7. Geological map of the eastern part of the Børgefjell window with the location of studied dykes in the Lower Allochthon, compiled from Foslie & Strand (1956), Gustavson (1973), Greiling (1988), Zachrisson (1991), and our data. See Figure 2 for location.

3.b. Middle Allochthon

3.b.1. Lower units of the Middle Allochthon

Mafic dykes have been observed in numerous tectonic slices or lenses of crystalline rocks, derived from the pre-Caledonian basement (M. A. Günther, unpub. Diploma thesis, Mainz Univ., 1984; Greiling, 1985; Zachrisson & Greiling, 1993, 1996). U–Pb zircon dating of a crystalline rock revealed a Palaeoproterozoic upper

recrystallized into an even-grained texture of albite, carbonate, biotite and opaque minerals. The latter show a preferred orientation approximately parallel with the upper margin. Sample G80143, width about 4.5 mm, crossed polarizers. (c) Remnants of primary plagioclase phenocrysts (diagonal and centre right) in a completely recrystallized matrix. The diagonally oriented 'phenocryst' shows an internal texture which resembles an S–C fabric and which documents relative movement along the long axis of the crystal during or after partial replacement by sericite. Sample G80140, width about 2.3 mm, crossed polarizers. (d) Dyke with foliation parallel with that of gneissic host-rock. (e) Well-preserved ophitic texture in the middle of a 30 m thick dyke, composed of pyroxene, plagioclase and minor opaque minerals. Both pyroxene and plagioclase show alterations along their margins with sericite and biotite as newly formed phases. Sample G8417, width 4.5 mm, crossed polarizers. (f) Remnants of ophitic texture from the margin of the dyke shown in (e). Relics of plagioclase phenocrysts show an open V shape in the middle. Plagioclase is completely replaced by sericite, carbonate, albite. In the matrix, additional secondary minerals include epidote, clinozoisite and opaque phases. The secondary minerals show a weak preferred orientation, approximately subvertical. Sample G8415, width 2.3 mm, plane polarized light. (g) Cataclastic and mylonitic texture showing polyphase shearing along subhorizontal and diagonal surfaces. Relatively coarse grains are composed of plagioclase, epidote, carbonate, chlorite. Sample G8428, width 4.5 mm, plane polarized light.

https://doi.org/10.1017/S0016756807003299 Published online by Cambridge University Press

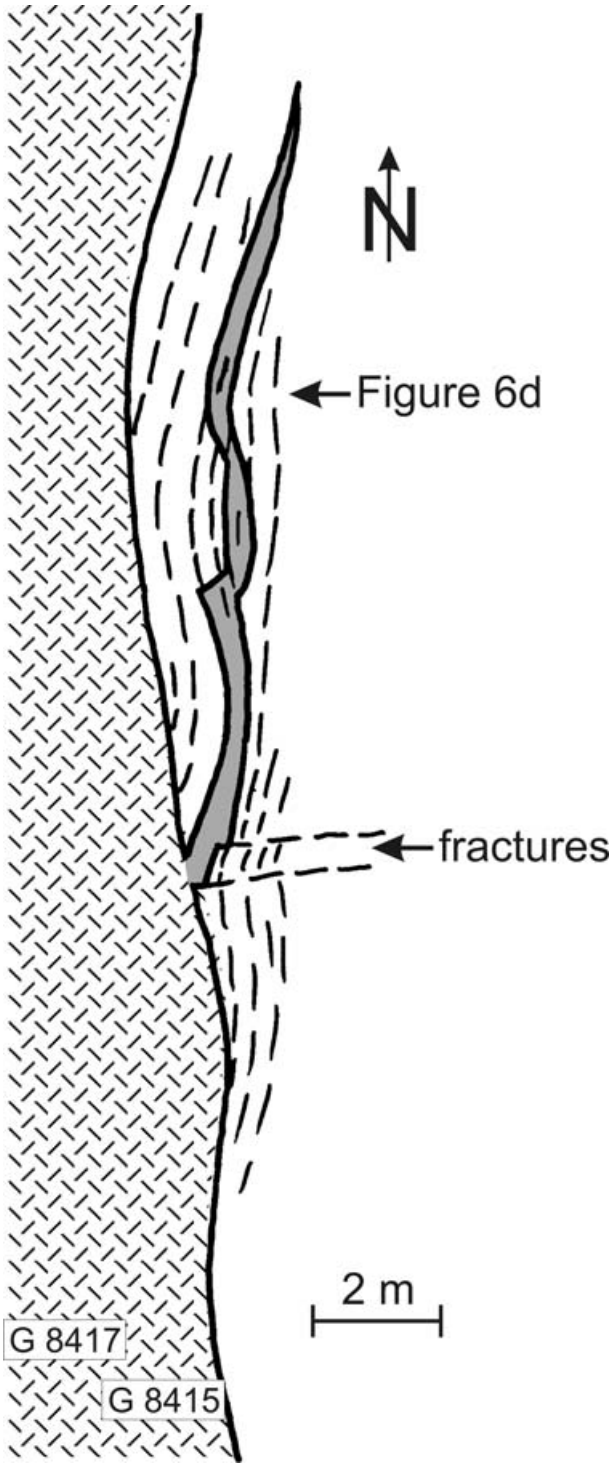

Figure 8. Plan view of subvertical dyke with thick, coarse-grained undeformed part and 'offshoot', which is subsequently foliated and sheared. Location is marked as G84:16–19 on Figure 7. For legend see Figure 4.

intercept age of 1766 Ma, similar to that of the country rocks in the Autochthon and Lower Allochthon, and a Grenvillian or Sveconorwegian lower intercept age of 1026 ± 79 Ma (Greiling, Stephens & Persson, 2002). This Grenvillian 'event' is probably related to shearing in the basement rocks. Since this shearing event also overprinted the mafic dykes (see below), the dykes must be older than *c.* 1026 Ma. This is also in agreement with the 1.26 Ga age of the mafic dykes of the Central Scandinavian Dolerite Group (Söderlund *et al.* 2005).

In low-strain domains, metre-thick dykes with patches of altered plagioclase phenocrysts can still be discerned; highly sheared dykes occur as centimetre-thin layers. In places, for example, at Grannäs (location on Fig. 2) and at Dikanäs (Fig. 9), dykes are clearly distinguishable by their fine grain size relative to the country rock, which is a foliated metagabbro. North of Bollvattnet (Fig. 9), a 1 m thick dyke is exposed in a coarse-grained gneiss. In the best-preserved, central part of the dyke, white patches in a dark grey-green groundmass can be discerned. These patches apparently represent remnants of primary plagioclase phenocrysts. Foliations in dyke and country rock are parallel with each other and with their contact surface planes (Fig. 10a). Ten metres along strike, the rocks are more strongly foliated, and the dyke width is reduced to 1–2 cm (Fig. 10b). Such a situation is typical and can be observed also in the other dykes of the Middle Allochthon. Microscopically, the foliation in the dykes shows more or less distinct cleavage domains, which enclose some less deformed microlithons. Minerals comprise mostly albite, epidote, clinozoisite, chlorite and opaques. In the less-deformed domains, albite–epidote pseudomorphs after plagioclase phenocrysts may be visible (Fig. 10c). However, the complete mineral assemblage is secondary and indicates lower greenschist-grade metamorphic conditions. This is also true for the more intensely foliated parts (Fig. 10d).

3.b.2. Särv Nappe equivalents

The Särv Nappe has been grouped earlier as the highest structural unit of the Middle Allochthon (Gee & Zachrisson, 1979). Dykes in the Särv Nappe have been well studied at their type area (Ottfjället; see Fig. 1 for location) and elsewhere in the Scandinavian Caledonides (e.g. Andreasson, 1994). Their age has been determined as *c.* 665 Ma (Claesson & Roddick, 1983). These Ottfjället dykes are exposed almost exclusively within arkoses and quartzites of Neoproterozoic age, and are distinct from the other mafic dykes of the Lower and Middle allochthons in their age and their geochemical composition. In order to document all of the Middle Allochthon dykes, the Särv-type dykes are briefly discussed here. They are also included in order to document that they are distinct from the other Middle Allochthon dykes, both with regard to their microtexture and their geochemistry (see Section 5.c.2).

In places where deformation intensity is low, it can be observed that the mafic dykes cut the bedding in the arkosic country rocks at a high angle, and they were

https://doi.org/10.1017/S0016756807003299 Published online by Cambridge University Press

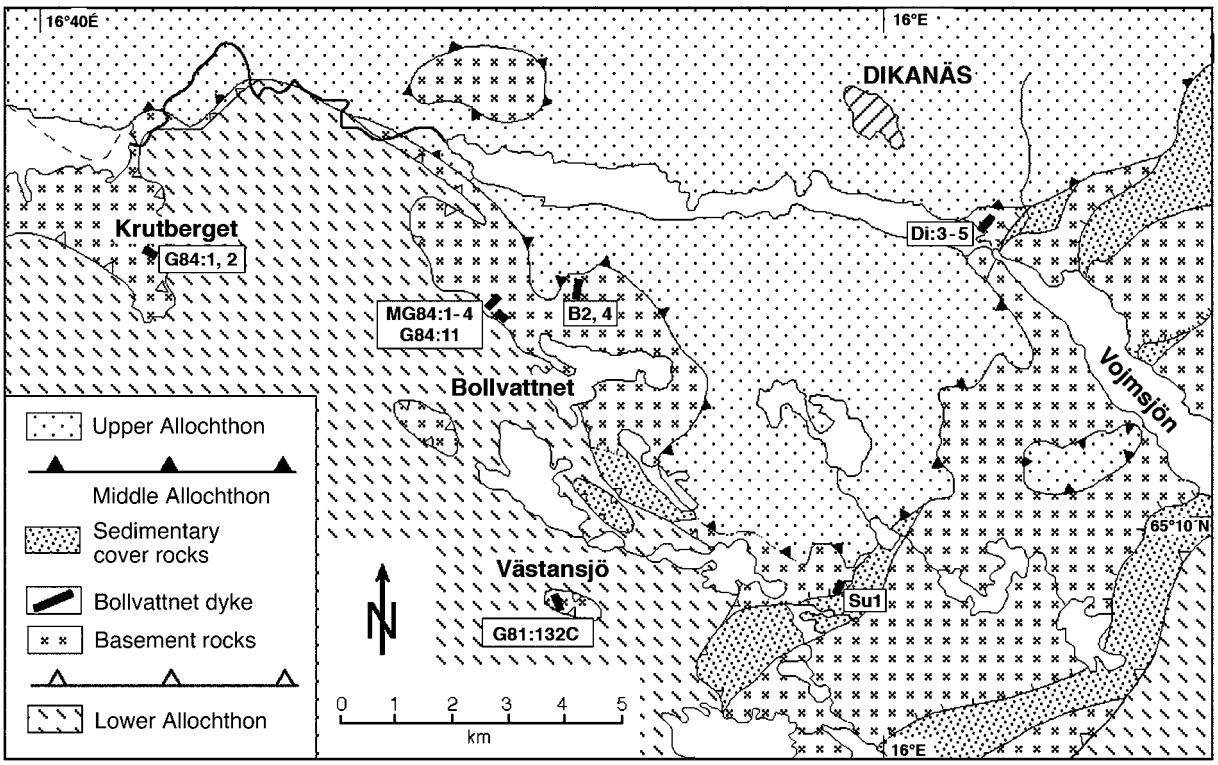

Figure 9. Geological map of the northwest part of the Stalon Nappe, Middle Allochthon, with the location of studied dykes, simplified from Zachrisson & Greiling (1993) and Greiling & Zachrisson (1999). Since the dyke exposures are grouped around Lake Bollvatnet, they are called here Bollvatnet dykes.

probably normal to the bedding, that is, vertical, in the original, undeformed state (e.g. Gee & Kumpulainen, 1980; Gilotti & Kumpulainen, 1986). Progressive deformation, mostly by simple shear, successively reduced the angle between bedding and dyke contact towards zero. This deformation is quite irregular and variable. Dykes which are clearly discordant retain most of their primary texture. Corresponding micrographs show a coarse, ophitic texture, dominated by plagioclase and pyroxene, which are partly replaced by albite and hornblende, respectively (Fig. 10e). This metamorphic overprint occurred without a change in the primary fabric, apparently as the product of a thermal event, which was not related to a deformation event. Those dykes which are sheared developed a foliation parallel with their margin and with the layering in the host rock arkoses. Microscopically, a static recrystallization is obvious, but the fabric mimics a planar foliation with alternating bands of relatively mafic (hornblende, biotite) and relatively felsic (plagioclase) character, respectively (Fig. 10f). Since the hornblende crystals do not show any internal strain, in spite of their strong preferred orientation, it is assumed that the hornblende recrystallized after the re-orientation, which produced the foliation. As a consequence, both the little-deformed and the strongly sheared dykes document a late thermal overprint. Such a thermal overprint has not been observed in all the other studied dykes.

4. Magnetic fabric analyses in the Central Scandinavian Dolerite Group

In order to assess the fabric changes of the mafic dykes together with changes in (magnetic) mineralogy during progressive deformation, the anisotropy of magnetic susceptibility (AMS) was measured with the help of a kappabridge KLY-2 (AGICO, Brno). AMS parameters used here are the mean susceptibility (K_{mean}), shape factor (T) and corrected anisotropy factor (P'). They are calculated following Jelinek (1981) or Tarling & Hrouda (1993), using the ANISO14 software package.

Selected samples from the Autochthon (Näverliden, Storuman; see Fig. 2), the Lower Allochthon (Bångonåive, Børgefjell; see Figs 2, 7) and the Middle Allochthon (Västansjö, Bollvattnet; see Fig. 9) are taken as examples. Characteristic values of the bulk susceptibility, shape and anisotropy, as well as the orientation of AMS principal axes, are reported in the following.

Bulk susceptibility is generally high in the dykes of the Autochthon and clearly indicates ferromagnetic behaviour of the samples. Magneto-mineralogical studies show 0.5 to 0.15 mm sized partly skeletal grains of Fe–Ti-oxides with ilmenite-lamellae (Fig. 11). In some samples a minor contribution of pyrrhotite is also observed (Kontny & de Wall, 2000, fig. 1a, p. 423). The course of temperature dependence of magnetic susceptibility clearly indicates magnetite as

https://doi.org/10.1017/S0016756807003299 Published online by Cambridge University Press

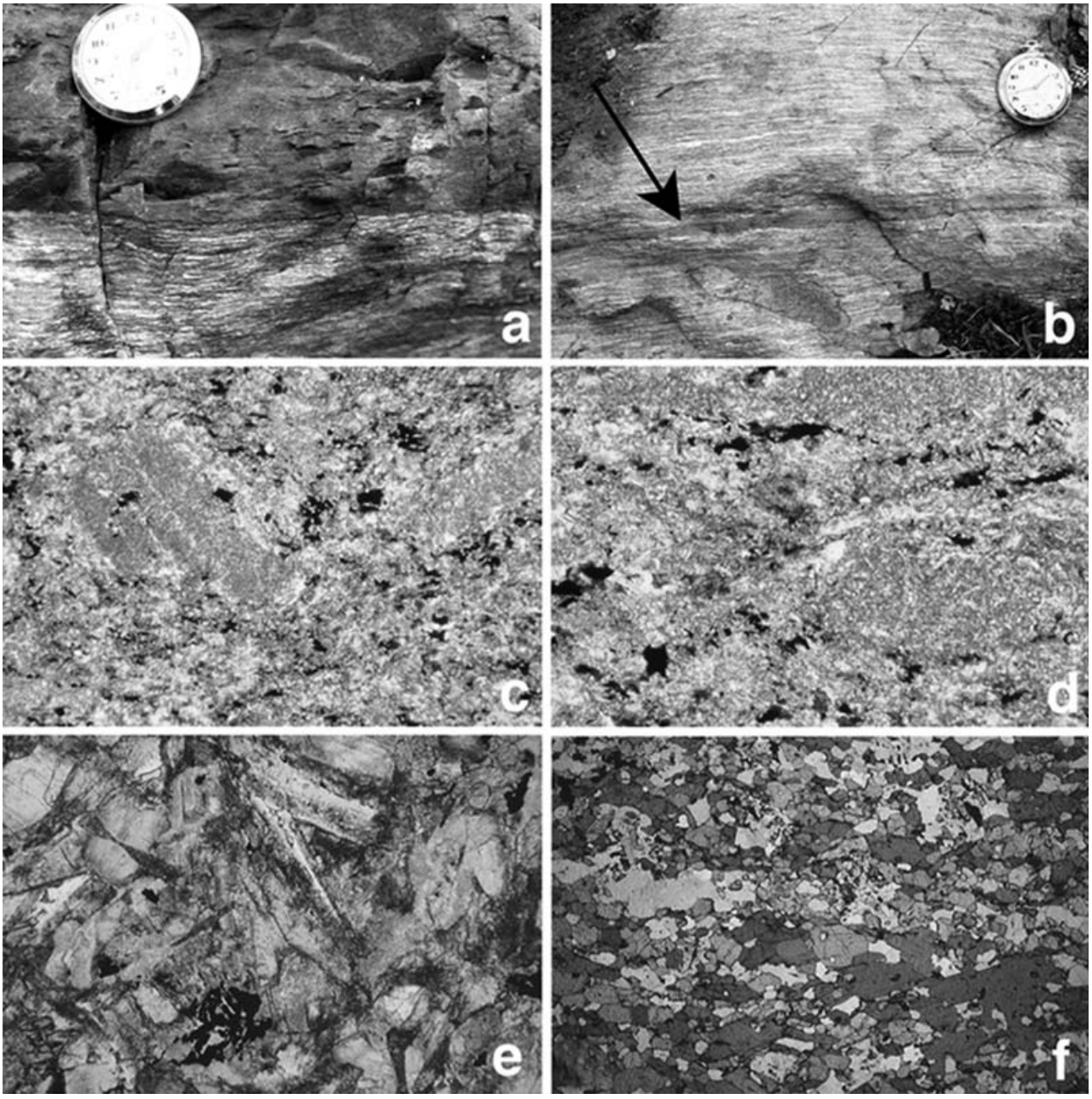

Figure 10. Field photograph and micrographs of (a–d) dykes in the Middle Allochthon, including (e, f) the Särv Nappe. (a) Contact of dyke against gneissic host rock. Note strong foliation in both rocks, subparallel with the contact. (b) 'Remnant' of dyke (arrow) within gneissic host rock, about 10 m along-strike from (a). Note foliation parallel with contacts and strongly reduced dyke thickness due to shearing. (c) Micrograph of mylonitic dyke rock with 'ghost' or pseudomorph of plagioclase phenocryst at right. The primary mineralogy of the rock is completely replaced by albite, carbonate, sericite, epidote, clinozoisite and opaque minerals. Sample G80132B, see location on Figure 9; width 2.3 mm, plane polarized light. (d) As (c), more strongly recrystallized and with a clear preferred orientation (subhorizontal). Sample G80132A, see location on Figure 9, width 1.1 mm, plane polarized light. (e) Well-preserved part of dyke in the Särv Nappe with coarse, ophitic texture. Plagioclase and pyroxene are partly replaced by secondary minerals. Sample E80145, width 2.3 mm, plane polarized light, location Vinevardo on Figure 2. (f) Särv Nappe dyke rock with statically recrystallized, undeformed secondary minerals albite, hornblende, biotite and minor opaque minerals. Note faint horizontal 'layering' and outsize biotite porphyroblasts at lower right. Sample E80147, width 4.5 mm, plane polarized light, location Vinevardo on Figure 2.

a ferromagnetic phase. The pronounced Hopkinson peak before reaching the Curie point is indicative of a significant contribution of single domain magnetite and can be related to the fine-grained magnetite that is intimately intergrown with titanite in the groundmass of the large oxide grains (Fig. 11b). Oxide assemblage and texture have been interpreted by Kontny & de Wall (2000) as formed under high-temperature (> 600 °C) conditions. The high bulk susceptibility is also responsible for the clear map-scale magnetic anomalies, which

https://doi.org/10.1017/S0016756807003299 Published online by Cambridge University Press

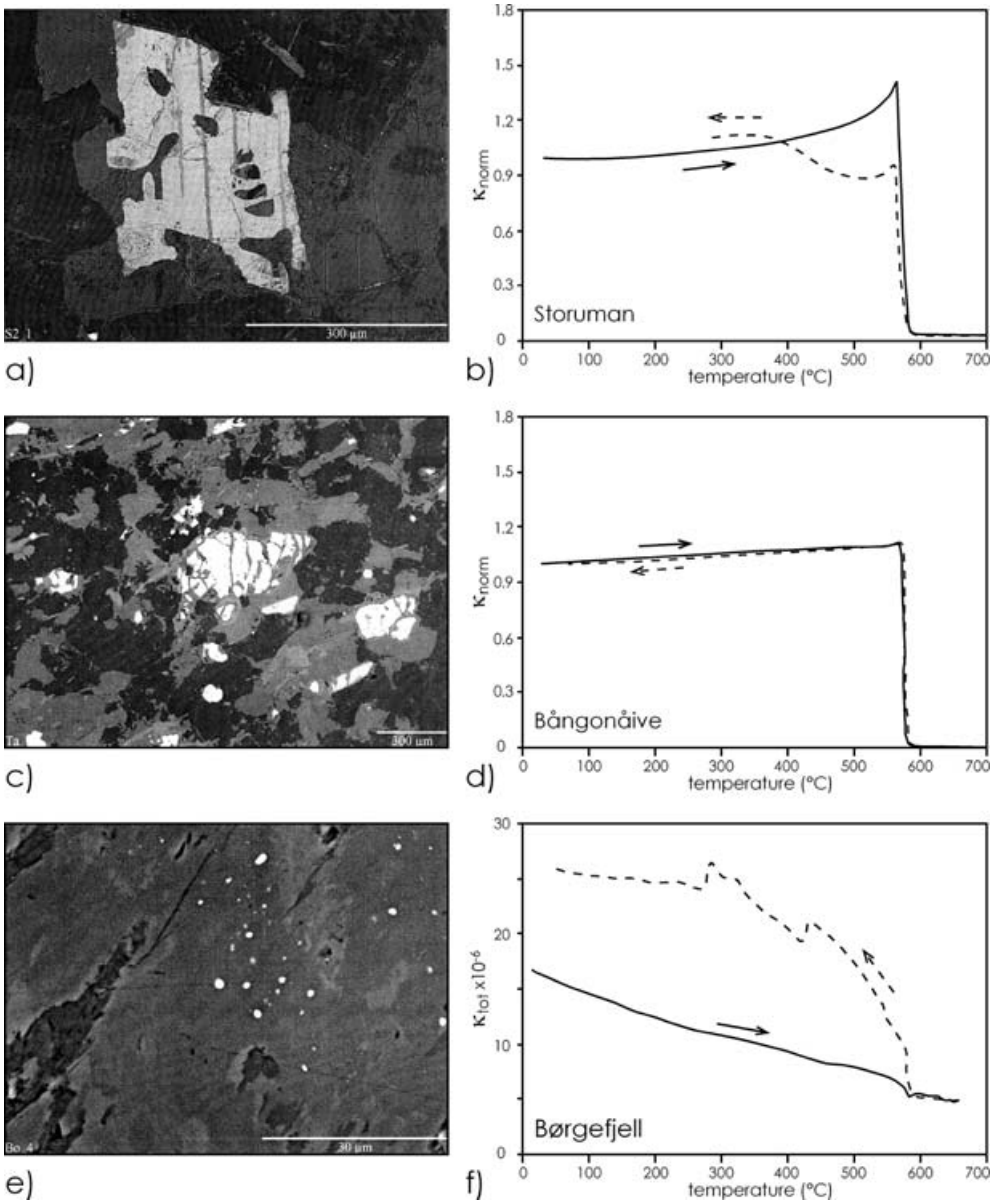

Figure 11. Magneto-mineralogical characteristics of dyke samples shown by backscattered images of Fe-oxides and temperature dependence of magnetic susceptibility (κ-T). In the undeformed dykes in the Autochthon, idiomorphic oxide grains with ilmenite laths are recognized (a). The κ-T behaviour with a distinct Hopkinson peak (b) is caused by fine-grained titanite/magnetite intergrowth. Elongated, locally cataclastic grains are found in dykes of the Lower Allochthon of the Bångonåive window (c), which are characterized by a multidomain magnetite curve of κ-T (d). (e) Fine-grained oxide relics in dykes from the Børgefjell window. κ-T behaviour is dominated by paramagnetic components and indicates a subordinate contribution of magnetite (f).

distinguish the dykes from their country rocks (Fig. 3; Björk, Kero & Zachrisson, 2000; Björk & Kero, 2002). It can be inferred that the AMS is mainly affected by the shape and distribution anisotropy of Fe-oxides. A wide scatter of oblate to prolate grains and anisotropy degrees of < 1.1 (Fig. 12) are in agreement with the general pattern of AMS in magmatic fabrics (Tarling & Hrouda, 1993). In such fabrics the contribution of distribution anisotropy dominates the effect of grain shape anisotropy (Hargraves, Johnson & Chan, 1991; Stephenson, 1994).

Dykes in the Proterozoic basement rocks of the Lower Allochthon show a transformation in their magneto-mineralogy as well as a modification of the magnetic fabric as a consequence of their incorporation in thrust units and the effects of nappe-stacking during Caledonian orogenic deformation. The dykes are characterized by a wide range in bulk susceptibility from 10^{-1} to 10^{-3} SI units related to variations in magnetite content. Dyke rocks of the Bångonåive window are characterized by relatively high susceptibilities in the range of 2×10^{-2} to 9×10^{-2} SI units. Traces of the primary magmatic fabric are still preserved but the mineral assemblage is adjusted to the lower greenschist-facies conditions prevalent in this part of the Lower Allochthon (compare Fig. 6b, c).

https://doi.org/10.1017/S0016756807003299 Published online by Cambridge University Press

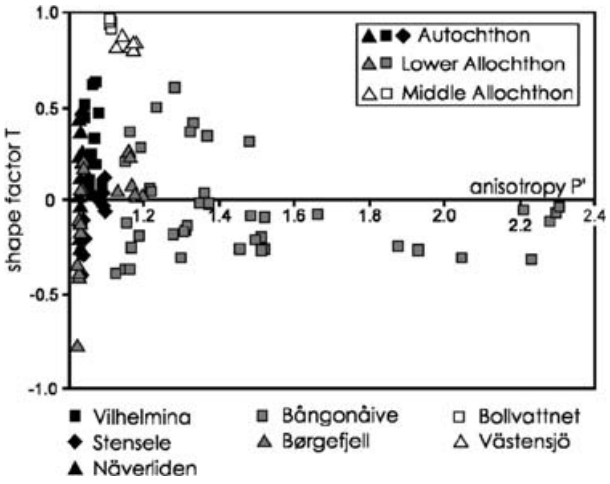

Figure 12. Shape and anisotropy of AMS presented in a Jelinek standard diagram (Jelinek, 1981; Tarling & Hrouda, 1993) for samples from the Autochthon, Lower Allochthon, and Middle Allochthon, respectively. For locations see Figures 2, 4, 7 and 9.

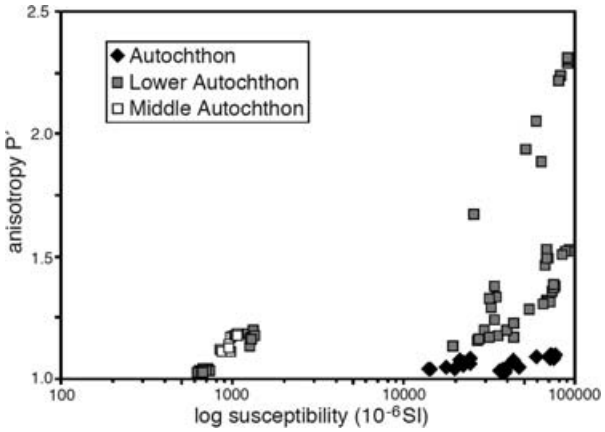

Figure 13. Anisotropy (P′) versus volume susceptibility presentation of AMS data suggests differences between magmatic fabric in the Autochthon (no correlation) and the deformation fabrics in the allochthonous units with distinct positive correlation.

Multidomain pure magnetite as an oxide phase has been inferred from rock-magnetic and thermomagnetic studies (de Wall & Greiling, 2000). Reflected light microscopy shows idioblastic magnetite and ilmenite intergrown with titanite and biotite (Kontny & de Wall, 2000, fig. 1b, p. 423). During progressive shearing, accompanied by retrograde metamorphic reactions, grain sizes of magnetite are reduced and volume susceptibilities decrease to values $< 10^{-3}$ SI. These values are measured in the Børgefjell dykes, which experienced a stronger overprint as compared to the dykes in the Bångonåive window described above. De Wall & Greiling (2000) report a distinct frequency dependence of magnetic susceptibility related to superparamagnetic behaviour of fine-grained magnetite, which can be regarded as relict grains. For the samples with susceptibilites $< 10^{-3}$ a predominance of paramagnetic subfabrics has to be considered.

Shape and anisotropy of the Bångonåive and Børgefjell samples show a wide range in anisotropies from < 1.1 to 2.4 (Fig. 12). A trend from variable shapes ranging from moderately oblate to moderately prolate ($T = +0.5$ to -0.5) for samples with lower anisotropies ($P' < 1.5$) to weakly linear in the samples with higher anisotropies is evident. In Figure 13 the anisotropy of AMS-ellipsoids, P' (corrected anisotropy factor: Jelinek, 1981), reflecting the eccentricity of the AMS-ellipsoid, is plotted versus the volume susceptibility. This diagram reveals the distinct difference between the magmatic fabric in samples from the Central Scandinavian Dolerite Group localities in the Autochthon and the deformation fabrics in the Lower Allochthon. In the magmatic fabrics the anisotropies are generally low and not affected by variations in volume susceptibility, whereas a clear positive correlation with increasing anisotropies at higher susceptibilities is present in the deformation fabrics. Anisotropies can exceed values of 2.4. Figure 13 clearly highlights the distinct difference between magmatic and deformation fabrics. This example also highlights the fact that the anisotropy of AMS-ellipsoids in deformed ferrimagnetic rocks does not give proper strain quantifications and cannot be used to evaluate the absolute magnitude of strain. The magnetic anisotropy in deformed ferrimagnetic rocks is determined by the distribution and the volume proportion of magnetically interactive grains (Hargraves, Johnson & Chan, 1991; Stephenson, 1994).

Samples from the highly sheared dykes from two localities of the Middle Allochthon are grouped in a well-defined field characterized by highly oblate shapes ($T > 0.8$) and low anisotropies ($P' < 1.2$). Volume susceptibilities are around 10^{-3} SI units, and the general trend of increasing anisotropy with increasing volume susceptibility (Fig. 13) points to a minor contribution of a ferrimagnetic phase to the magnetic fabric. In both localities, dykes are highly sheared and the internal foliations in the dyke are parallel with the deformation fabric in the host rocks. Magnetic fabric indicates that this shear fabric is strongly planar.

A common structural feature of all samples from dykes in the allochthonous units is a NW-trending magnetic lineation (Fig. 14a, b). This direction is in agreement with field measurements in the host rocks (Fig. 14c) and reflects the direction of tectonic transport in the Caledonian nappe units (e.g. Gayer & Greiling, 1989; Greiling, Garfunkel & Zachrisson, 1998). Surprisingly, the same trend of lineation is seen also in the magnetic fabric of the investigated autochthonous dyke and sill localities outside the present Caledonian belt. The magnetic lineation in the Autochthon could either reflect the magma flow direction in the intrusions or be interpreted as a Caledonian tectonic overprint.

https://doi.org/10.1017/S0016756807003299 Published online by Cambridge University Press

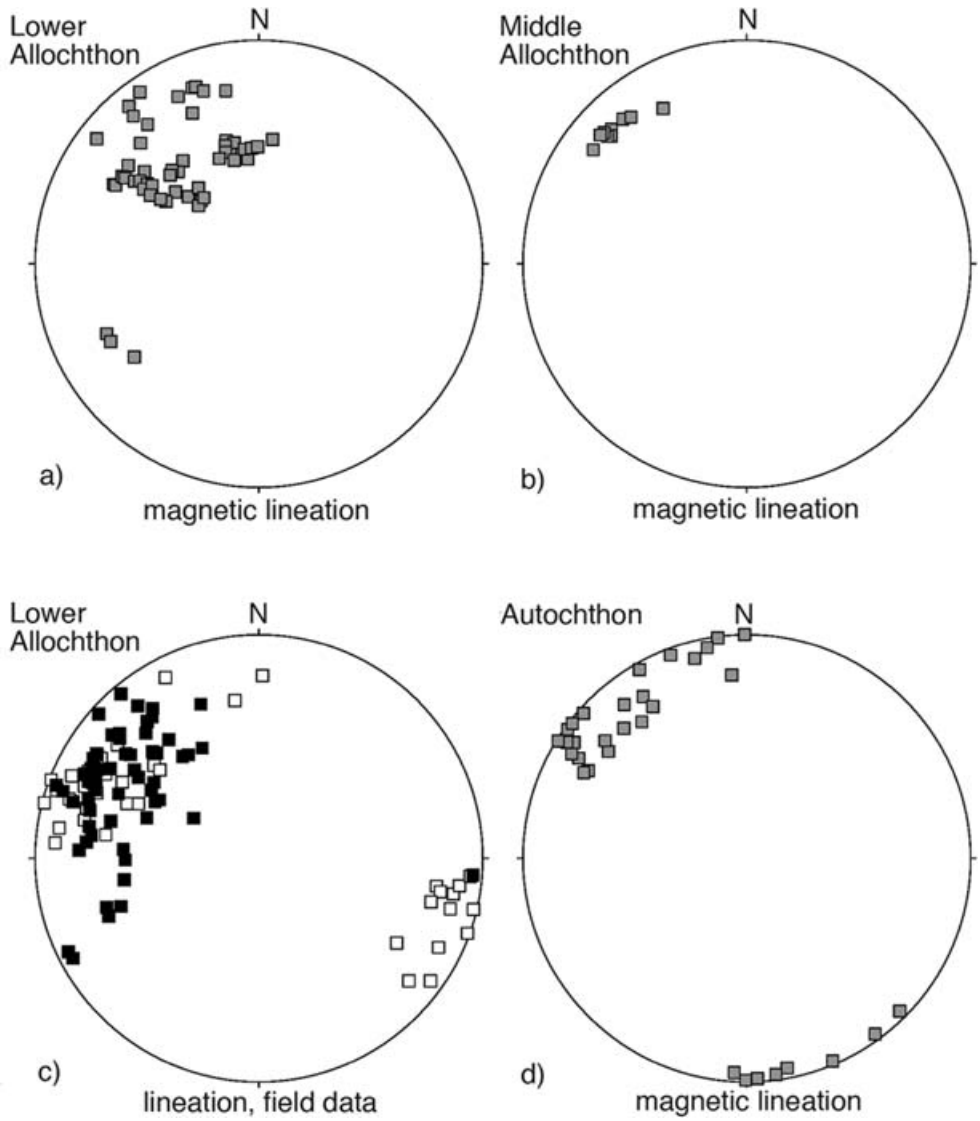

Figure 14. Shallow, NW-plunging magnetic lineations (long axis of AMS-ellipsoid) in dykes from the Lower Allochthon (a) and the Middle Allochthon (b) crystalline units correspond to the orientation of lineations measured in the field from crystalline parts of the Caledonian thrust units (Bångonåive, filled squares; Børgefjell, open squares) (c). In contrast, NW trends of magnetic lineations in dykes of the Autochthon (d) may be interpreted as magmatic flow direction.

Our anisotropy data (Fig. 14d) point to a magmatic flow fabric and do not support an interpretation in terms of tectonic influence. The orientation of AMS axes in Storuman and Näverliden indicates a shallow NW-dipping magnetic foliation (plane which includes maximum and intermediate axes of AMS-ellipsoids) and a magnetic lineation (long axis of AMS-ellipsoids) in dip direction. An interpretation in terms of normal magnetic fabric where magnetic foliation is parallel to the boundary of dykes and sills (e.g. Knight & Walker, 1988; Rochette, Jackson & Aubourg, 1991; Tarling & Hrouda, 1993) is consistent with a model of shallow dipping intrusions (sills) and a NW to SE magma flow direction. Such a model implies that a potential mantle plume area was oriented towards the northwest (in present coordinates).

5. Geochemistry

In order to characterize the studied mafic dykes geochemically, 91 samples from 36 locations have been analysed for major elements and 79 of them also for their trace elements (Table 1). The samples comprise mafic dykes from the autochthonous Fennoscandian Shield (Västerbotten complex) and allochthonous crystalline basement rocks from the Caledonian Lower and Middle allochthons. An early batch of samples was analysed by XRF methods, with major elements from glass beads and trace elements on powder pellets at the Institute of Geosciences, Mainz University, Germany. These samples documented preliminary results on the distribution of dykes (Greiling *et al*. 1984) but details have not yet been published. During subsequent

https://doi.org/10.1017/S0016756807003299 Published online by Cambridge University Press

Table 1. Major and trace element contents of mafic dykes from different tectonic units

Unit	AUT	AUT	AUT	AUT	AUT	AUT	AUT	AUT	AUT	AUT	AUT	AUT	AUT	AUT	AUT	AUT	AUT
Sample no.	G80: 154	G80: 155	G80: 156	S1	S2	S2A	S2A-1	G95:N1A	G95:Ly1A	G95:Ly2A	G95:Ly3	G95:Ly3A	G84: 31	G84: 32	G84: 34	G84: 35	G84: 36
Locality	Umeälven	Umeälven	Umeälven	Umeälven	Umeälven	Umeälven	Umeälven	Näverliden	Orrkulla	Orrkulla	Orrkulla	Orrkulla	Granberget	Granberget	Granberget	Granberget	Granberget
Map sheet	23H Stensele	23H Stensele	23H Stensele	23H Stensele	23H Stensele	23H Stensele	23H Stensele	22I Lycksele	22I Lycksele	22I Lycksele	22I Lycksele	22I Lycksele	22G Vilhelmina	22G Vilhelmina	22G Vilhelmina	22G Vilhelmina	22G Vilhelmina
Coordinates	7219 080	7219 080	7219 080	7219 080	7219 080	7219 080	7219 080	7172 450	7164 400	7164 400	7164 400	7164 400	7169 500	7169 500	7169 500	7169 500	7169 500
	1561 030	1561 030	1561 030	1561 030	1561 030	1561 030	1561 030	1611 000	1625 200	1625 200	1625 200	1625 200	1545 550	1545 550	1545 550	1545 550	1545 550
SiO_2	44.01	44.19	41.40	44.30	43.90	45.35	45.17	46.67	44.34	45.77	45.90	45.86	44.74	45.07	44.84	44.61	45.00
TiO_2	3.19	3.01	3.14	3.39	3.47	3.50	3.51	2.72	1.91	1.82	1.78	1.78	3.28	3.29	3.24	3.05	0.96
Al_2O_3	15.96	17.17	16.21	14.70	15.00	15.79	15.74	15.40	15.81	15.26	15.08	15.01	15.31	15.33	15.34	15.27	14.90
Fe_2O_3	4.36	4.73	4.85	16.13	14.76	14.52	14.65	15.92	15.10	14.43	15.14	15.11	16.61	16.91	16.72	16.25	9.90
FeO	10.98	10.37	10.45														
MnO	0.25	0.25	0.27	0.19	0.23	0.29	0.29	0.22	0.20	0.20	0.21	0.21	0.21	0.20	0.22	0.18	0.18
MgO	4.96	4.76	4.64	6.38	5.72	4.94	4.94	5.81	8.71	8.70	9.81	9.85	5.57	5.63	5.89	6.09	9.97
CaO	7.60	8.11	7.52	8.02	7.64	7.78	7.77	8.36	7.41	9.17	8.70	8.70	7.94	8.02	7.98	7.80	9.13
Na_2O	3.54	3.33	4.33	3.00	3.30	3.63	3.60	3.11	2.22	2.44	2.52	2.57	3.16	3.44	3.44	3.33	3.06
K_2O	1.17	1.48	2.04	1.24	1.20	1.26	1.25	1.42	1.68	0.78	0.73	0.73	1.39	1.33	1.34	1.27	2.46
P_2O_5	0.75	0.89	0.82	0.73	0.85	0.76	0.74	0.60	0.41	0.35	0.36	0.36	0.73	0.76	0.72	0.69	0.50
LOI	3.08	2.37	3.42										0.95	0.15	0.38	1.52	4.05
Total	99.85	100.66	99.09	98.08	96.07	97.82	97.66	100.23	97.80	98.92	100.23	100.18	99.89	100.13	100.11	100.06	100.11
Ba													650	744	761	786	2579
Cr	37	38	35	43	42								46	49	46	40	264
Nb	12	11	13	12	13		13	12	7	6	7		12	12	12	12	42
Ni	68	73	71	68	68								84	85	96	111	168
Rb	30	32	63	28	43								39	23	25	27	79
Sr	476	475	470	499	453								447	467	481	476	1231
Y	39	39	38	37	39		43	45	24	23	25		36	36	36	36	19
Zr	169	176	174	184	192		182	229	119	104	113		167	172	169	162	216

Unit	AUT	AUT	AUT	AUT	AUT	AUT	AUT	AUT	AUT	AUT	AUT	AUT	AUT	AUT	AUT	AUT
Sample no.	V1	V1A-1	V1A-2	V1-b	V4	V4a	V6	G96:1, DoA	G96:11A-1	G96:11A-2	G96:12A-1	G96-12A-2	G96–15A-1	G96–15A-2	G96–16A-1	G96–16A-2
Locality	Granberget	Granberget	Granberget	Granberget	Granberget	Granberget	Granberget	Mårdsjöberget	Brattforsberget	Brattforsberget	Brattforsberget	Brattforsberget	Miltallberget	Miltallberget	Återskallberget	Återskallberget
Map sheet	22G Vilhelmina	22G Vilhelmina	22G Vilhelmina	22G Vilhelmina	22G Vilhelmina	22G Vilhelmina	22G Vilhelmina	21G Dorotea	21G Dorotea	21G Dorotea	21G Dorotea	21G Dorotea	21G Dorotea	21G Dorotea	21G Dorotea	21G Dorotea
Coordinates	7169 600	7169 600	7169 600	7169 600	7169 600	7169 600	7169 600	7132 850	7102 550	7102 550	7102 550	7102 550	7104 950	7104 950	7113 550	7113 550
	1545 150	1545 150	1545 150	1545 150	1545 150	1545 150	1545 150	1539 250	1522 200	1522 200	1522 200	1522 200	1522 250	1522 250	1523 800	1523 800
SiO_2	43.79	43.71	43.49	46.20	44.94	44.74	47.20	49.30	53.58	53.37	54.21	53.98	52.12	52.50	48.70	48.66
TiO_2	3.75	3.75	3.75	0.88	3.39	3.39	0.67	1.26	1.57	1.57	1.63	1.61	1.07	1.07	1.17	1.17
Al_2O_3	15.04	15.04	14.91	13.50	15.53	15.45	13.60	15.85	15.00	14.89	15.36	15.19	16.04	16.06	16.54	16.58
Fe_2O_3	16.81	16.76	16.78	11.52	16.56	16.54	10.58	12.99	12.35	12.32	12.48	12.48	11.05	11.08	9.22	9.21
FeO																
MnO	0.27	0.27	0.27	0.18	0.21	0.21	0.16	0.16	0.21	0.21	0.21	0.21	0.16	0.17	0.14	0.14
MgO	5.25	5.26	5.22	10.88	5.21	5.17	11.62	6.90	3.11	3.08	3.19	3.18	6.13	6.17	7.33	7.32
CaO	8.66	8.62	8.63	8.28	8.13	8.12	7.72	8.46	7.02	7.01	6.49	6.48	7.79	7.80	7.18	7.19
Na_2O	2.75	2.73	2.71	2.20	3.26	3.27	2.28	3.44	3.65	3.70	3.75	3.73	1.33	1.37	4.57	4.60
K_2O	1.22	1.22	1.21	1.38	1.33	1.34	1.54	0.61	1.61	1.61	2.07	2.07	2.51	2.51	2.05	2.03
P_2O_5	0.71	0.68	0.69	0.18	0.75	0.75	0.25	0.14	0.94	0.92	0.96	0.95	0.23	0.24	0.52	0.52
LOI																
Total	98.25	98.04	97.65	95.20	99.31	98.98	95.62	99.11	99.05	98.69	100.35	99.88	98.44	98.97	97.41	97.42
Ba																
Cr				301	27		306									
Nb				12	14		12	9	12		12		6		35	
Ni				131			134									
Rb				57			62									
Sr				443			506									
Y				22	40		16	20	39		41		30		23	
Zr				117	180		105	74	163		166		94		90	

Table 1. *(Contd.)*

Unit	LA	LA	LA	LA	LA	LA	LA	LA	LA	LA	LA	LA
Sample no.	G78: 18	G80: 140	G80: 141	G80: 143	G80: 144	G81: 64	G81: 65	G81: 67	T1-g (dW)	T4-c (dW)	E80:S1	G84: 16
Locality	Tärnaån	Tärnaån	Tärnaån	Tärnaån	Tärnaån	Tärnaån	Tärnaån	Tärnaån	Tärnaån	Tärnaån	Vuollelite	Jetneme
Map sheet	24F Tärna	24F Tärna	24F Tärna	24F Tärna	24F Tärna	24F Tärna	24F Tärna	24F Tärna	24F Tärna	24F Tärna	23F Fatmomakke	2025 III Ranseren
Coordinates	7296 300	7296 280	7296 280	7296 300	7296 300	7296 300	7296 300	7296 300	7296 300	7296 300	7201 140	N 20200
	1483 180	1483 150	1483 150	1483 180	1483 180	1483 180	1483 180	1483 180	1483 180	1483 180	1489 000	E 66550
SiO_2	50.20	52.57	49.96	52.87	51.96	51.91	50.44	51.32	51.30	51.70	46.78	47.58
TiO_2	1.96	1.87	1.76	1.89	1.87	1.95	1.97	1.93	1.93	1.86	1.34	1.36
Al_2O_3	15.39	15.69	14.59	16.86	16.86	15.27	15.16	15.27	15.20	15.60	17.21	16.07
Fe_2O_3	5.23	4.54	4.42	4.13	4.13	4.59	4.46	4.39	11.17	10.67	3.23	12.12
FeO	6.34	5.88	5.95	5.93	6.16	6.12	6.66	6.36			8.90	
MnO	0.20	0.22	0.21	0.22	0.23	0.17	0.17	0.24	0.17	0.18	0.27	0.17
MgO	4.57	4.10	4.03	4.06	4.15	4.07	4.58	4.12	4.55	4.24	5.38	7.20
CaO	6.28	5.78	6.49	5.81	5.85	5.93	6.18	5.97	6.25	5.94	8.67	10.06
Na_2O	4.51	4.03	4.06	3.99	3.92	4.20	4.57	4.04	3.80	3.90	3.14	1.95
K_2O	2.90	3.42	2.84	3.45	3.22	3.18	2.54	3.13	2.86	2.99	1.18	1.04
P_2O_5	1.26	1.31	1.29	0.70	0.89	0.78	1.24	1.15	1.33	1.30	0.42	0.20
LOI	0.25	2.08	3.05	1.21	1.64	0.71	1.35	1.10			2.93	2.56
Total	98.84	99.41	95.60	99.91	99.24	98.17	97.97	97.92	98.56	98.38	99.45	100.31
Ba												287
Cr	60					42	59	46	90	76		127
Nb		14	15	15	16	15	16	14	15	14	8	90
Ni		37	40	38	40				33	32	37	
Rb	80	58	65	54	63	55	53	63	56	63	25	40
Sr	804	775	723	818	798	786	629	756	817	780	714	343
Y	37					38	36	39	36	35	35	26
Zr	193	183	185	175	185	196	193	191	211	214	47	84

Unit	LA	LA	LA	LA	LA	LA	LA	LA	LA	LA	LA	LA
Sample no.	G84: 18	G84: 19	G84: 16	G84: 18	G84: 19	G84: 22	G84: 23	G84: 24	G84: 26	G84: 27	Bo1	G78:44
Locality	Jetneme	Jetneme	Jetneme	Jetneme	Jetneme	Jetnamsklumpen	Jetnamsklumpen	Jetnamsklumpen	Vueperetjahke	Vueperetjahke	Jetneme	Rotnan
Map sheet	2025 III Ranseren	2025 III Ranseren	2025 III Ranseren	2025 III Ranseren	2025 III Ranseren	1925 II Börgefjellet	1925 II Börgefjellet	1925 II Börgefjellet	2025 III Ranseren	2025 III Ranseren	2025 III Ranseren	2025 III Ranseren
Coordinates	N 20200	N 20200	N 20200	N 20200	N 20200	N 22950	N 22950	N 22950	N 18800	N 18800	N 20200	N 33060
	E 66550	E 66550	E 66550	E 66550	E 66550	E 62850	E 62850	E 62850	E 63400	E 63400	E 66550	E 63900
SiO_2	47.86	47.81	47.58	47.86	47.81	48.79	44.83	48.53	45.52	44.78	45.90	42.91
TiO_2	1.36	1.31	1.36	1.36	1.31	2.23	2.56	2.24	3.06	3.10	1.30	2.79
Al_2O_3	16.30	16.31	16.07	16.30	16.31	14.27	15.62	14.18	15.51	15.51	15.40	16.11
Fe_2O_3	12.34	12.13	12.12	12.34	12.13	14.85	15.62	14.37	14.09	14.07	12.11	4.92
FeO												10.01
MnO	0.19	0.19	0.17	0.19	0.19	0.20	0.13	0.22	0.22	0.17	0.17	0.26
MgO	7.30	7.61	7.20	7.30	7.61	5.78	9.65	6.30	5.93	5.29	8.88	6.40
CaO	9.90	9.85	10.06	9.90	9.85	8.49	2.42	7.99	3.99	5.28	9.98	8.65
Na_2O	2.41	2.62	1.95	2.41	2.62	2.66	2.12	2.76	2.63	2.93	2.30	3.55
K_2O	0.97	0.66	1.04	0.97	0.66	1.44	1.78	1.46	5.66	5.11	0.66	1.00
P_2O_5	0.19	0.19	0.20	0.19	0.19	0.32	0.34	0.33	1.12	0.97	0.16	0.67
LOI	1.05	1.33	2.56	1.05	1.33	1.11	4.88	1.61	2.48	2.77		1.34
Total	99.85	100.00	100.31	99.85	100.00	100.14	99.96	99.99	100.11	99.97	99.97	98.61
Ba	400	274	287	400	274	340	202	337	628	708		
Cr	113	117	127	113	117	159	198	153	33	75	113	
Nb	120	155	90	120	155	50	67	65	39	52	143	10
Ni												
Rb	25	19	40	25	19	84	108	88	447	386	14	21
Sr	350	330	343	350	330	267	42	250	189	285	367	477
Y	24	23	26	24	23	44	45	45	47	36	21	34
Zr	86	84	84	86	84	201	215	200	237	207	80	146

Table 1. *(Contd.)*

Unit	MA	MA	MA	MA	MA	MA	MA	MA	MA	MA	MA	MA-Särv	MA-Särv	MA-Särv
Sample no.	G84: 1	G84: 2	G84: 11	MG84: 01	MG84: 02	MG84: 03	G81: 132C	MG84: 04	B2	B4	Su1	G80: 115	G80: 118	G80: 120
Locality	V. Krutberget	V. Krutberget	Bomanstjärnen	Bomanstjärnen	Stortjärnen	Stortjärnen	Västansjö	Stortjärnen	Bollvattnet	Bollvattnet	Sutsberg	Lövberg	Rammelknulen	Rammelknulen
Map sheet	23F Fatmomakke	23F Fatmomakke	23G Dikanäs	23G Dikanäs	23G Dikanäs	23G Dikanäs	23G Dikanäs	23G Dikanäs	23G Dikanäs	23G Dikanäs	23G Dikanäs	22F Risbäck	22F Risbäck	22F Risbäck
Coordinates	7234 520	7234 520	7233 860	7233 860	7233 360	7233 400	7227 830	7233 280	7233 840	7233 840	7228 430	7178 030	7178 760	7179 240
	1490 160	1490 160	1503 250	1503 250	1501 690	1501 650	1502 950	1501 700	1503 530	1503 530	1508 340	1475 220	1474 040	1473 630
SiO_2	45.74	53.21	46.71	46.93	44.01	44.77	48.68	45.01	45.40	45.90	42.00	48.81	50.00	45.95
TiO_2	1.31	1.04	2.53	267	2.48	3.08	1.76	2.73	2.20	2.61	1.34	1.22	1.21	1.15
Al_2O_3	15.89	18.41	14.97	14.63	13.06	14.73	17.55	14.46	13.10	13.20	13.90	15.91	13.48	16.43
Fe_2O_3	11.28	8.00	14.92	15.38	14.97	15.90	4.19	14.36	14.37	15.24	14.08	3.06	1.78	2.44
FeO							6.65					6.66	7.31	6.73
MnO	0.15	0.10	0.25	0.26	0.25	0.26	0.13	0.22	0.22	0.23	0.20	0.19	0.20	0.18
MgO	8.28	3.33	5.88	5.82	9.85	5.10	5.12	7.38	7.55	6.32	10.10	7.83	10.60	7.36
CaO	9.84	5.17	8.65	8.78	10.55	8.23	6.84	10.86	8.50	8.68	10.45	11.35	9.49	12.04
Na_2O	2.73	5.20	2.68	2.57	1.28	2.96	4.37	1.64	2.20	2.50	1.90	2.18	2.45	1.88
K_2O	2.34	3.55	1.25	1.22	1.25	1.34	2.09	1.01	1.36	1.24	1.75	0.48	1.05	0.55
P_2O_5	0.49	0.71	0.49	0.52	0.33	1.05	0.29	0.37	0.46	0.54	0.30	0.24	0.19	0.17
LOI	1.93	1.31	1.67	1.43	2.04	2.58	1.94	2.13				3.03	2.52	3.68
Total	99.98	100.03	100.00	100.21	100.07	100.00	99.61	100.17	95.36	96.46	96.02	97.93	97.76	94.88
Ba	677	791	453	427	654	716	967	529						201
Cr	75	20	143	130	328	62	113	175	149	123	84			299
Nb	10	21	22	20	22	9	12	25	18	23	6	11	9	8
Ni	96	22	128	119	259	66	73	140	125	116	102	47	218	82
Rb	62	117	25	26	19	28	39	16	31	29	27	13	36	18
Sr	1099	762	397	380	540	662	708	905	439	441	637	225	155	232
Y	21	28	58	58	22	41	35	25	52	63	24	27	22	22
Zr	98	122	288	296	153	154	371	167	276	311	76	82	78	81

Unit	MA-Särv	MA-Särv	MA-Särv	MA-Särv	MA-Särv	MA-Särv	MA-Särv	MA-Särv	MA-Särv	MA-Särv	MA-Särv	MA-Särv	MA-Särv	MA-Särv
Sample no.	G80: 121	G80: 122	G80: 124	G80: 125	G80: 127	G80: 134	G80: 134B	Sx2	Sx3	E80: 141	E80: 142	E80: 144	E80: 145	E80: 146
Locality	Rammelknulen	Rammelknulen	Rammelknulen	Solberg	Solberg	Skrymliden	Skrymliden	Saxnäs-Lillberget	Saxnäs-Lillberget	Vinevardo	Vinevardo	Vinevardo	Vinevardo	Vinevardo
Map sheet	22F Risbäck	22F Risbäck	22F Risbäck	22F Risbäck	22F Risbäck	22F Risbäck	22F Risbäck	23F Fatmomakke	23F Fatmomakke	23F Fatmomakke	23F Fatmomakke	23F Fatmomakke	23F Fatmomakke	23F Fatmomakke
Coordinates	7179 240	7179 420	7180 060	7190 450	7190 450	7183 630	7183 630	7205600	7205600	7202 650	7202 650	7202 490	7202 490	7202 490
	1473 630	1473 510	1473 270	1471 450	1471 450	1468 670	1468 670	1475500	1475500	1480 280	1480 280	1480 260	1480 260	1480 260
SiO_2	46.04	47.98	49.98	43.26	49.48	50.01	50.62	49.40	49.20	49.54	48.35	51.98	50.89	49.56
TiO_2	1.30	1.19	1.18	1.08	1.09	1.26	1.10	1.16	0.93	1.47	1.50	0.98	1.24	1.15
Al_2O_3	16.14	15.18	14.43	21.23	16.52	14.63	16.15	13.30	15.60	15.61	13.21	14.65	15.59	15.55
Fe_2O_3	1.99	1.86	1.79	1.97	1.69	2.38	1.87	10.79	9.03	2.14	2.61	2.55	1.19	2.29
FeO	6.62	6.71	7.27	6.76	6.77	7.45	6.77			7.36	8.59	8.40	8.20	7.43
MnO	0.18	0.18	0.16	0.17	0.17	0.20	0.18	0.17	0.13	0.19	0.22	0.27	0.20	0.19
MgO	7.56	6.29	7.85	10.93	7.16	7.15	7.74	8.91	9.04	7.96	7.43	6.76	6.96	7.68
CaO	11.26	10.19	11.27	9.86	10.47	10.7	10.80	11.37	12.11	12.14	11.46	10.45	10.97	10.89
Na_2O	1.96	1.69	2.40	2.25	2.08	3.23	2.44	2.40	2.30	2.32	2.46	2.19	2.12	2.08
K_2O	0.88	1.06	2.40	0.65	0.54	0.61	0.89	0.28	0.22	0.35	0.34	0.58	0.32	0.78
P_2O_5	0.18	0.19	0.18	0.23	0.17	0.19	0.18	0.12	0.08	0.18	0.20	0.19	0.18	0.16
LOI	4.93	5.14	2.04	2.20	2.69	2.84	2.05							
Total	94.11	92.52	98.91	98.39	96.14	97.81	98.74	97.90	98.64	99.26	96.37	99	97.86	97.76
Ba					178	149					79			
Cr		365			446	176		225	294		209			
Nb	9	7	11		9	9	10	8	6	12	11	12	9	6
Ni	66	75	38		81	45	97	85	75	91	55	27	72	51
Rb	13	43	16		18	16	25	6	5	7	12	7	7	8
Sr	251	271	240		221	174	246	193	197	246	215	177	194	198
Y	21	22	24		21	25	24	24	20	21	24	29	23	24
Zr	68	71	85		89	98	81	73	61	77	103	109	79	68

Table 1. *(Contd.)*

Unit	MA-Särv	MA-Särv	MA-Särv	MA-Särv	MA-Särv	MA-Särv
Sample no.	E80: 147	E80: 149	E80:150	E80:151	K2	G78: 22
Locality	Vinevardo	Vinevardo	Vinevardo	Vinevardo	Kultsjön	Njereutjakke
Map sheet	23F Fatmomakke	23F Fatmomakke	23F Fatmomakke	23F Fatmomakke	23F Fatmomakke	24F Tärna
Coordinates	7202 490	7202 560	7202 560	7202 560	7210200	7298 580
	1480 260	1480 260	1480 260	1480 260	1473150	1486 060
SiO_2	50.29	48.99	49.84	50.31	47.70	47.92
TiO_2	1.81	1.01	1.54	1.49	1.24	1.50
Al_2O_3	14.70	15.98	16.27	14.28	14.40	15.87
Fe_2O_3	3.36	3.38	1.72	1.64	10.19	4.91
FeO	8.21	8.32	9.56	8.97		7.96
MnO	0.24	0.18	0.24	0.22	0.15	0.27
MgO	5.70	6.63	5.63	6.60	9.94	6.29
CaO	10.21	10.65	9.95	10.89	9.46	6.53
Na_2O	2.47	2.53	2.43	2.47	2.10	4.02
K_2O	0.98	0.47	0.47	0.44	1.27	0.26
P_2O_5	0.21	0.21	0.22	0.20	0.09	0.16
LOI						2.86
Total	98.18	98.35	97.87	97.51	96.54	95.69
Ba	60					
Cr	87				477	
Nb	11	10		10	7	10
Ni	27	17		45	193	
Rb	17	11		9	41	6
Sr	164	218		205	210	218
Y	31	30		28	32	30
Zr	119	101		100	130	104

Major element oxide contents are given in weight %, trace element contents in ppm. AUT – Autochthon; LA – Lower Allochthon; MA – lower units of Middle Allochthon; MA-Särv – Särv-nappe equivalents. Coordinates refer to the Swedish grid. Map sheets Ranseren and Børgefjell are in Norway and coordinates thus refer to the Norwegian grid.

detailed mapping, mafic dykes were sampled, in order to obtain a comprehensive and representative coverage of analyses. These latter samples were analysed by ICP methods at ACME, Vancouver, Canada. All results were checked against international standards.

5.a. Autochthon dykes

The analysed 33 samples from nine locations represent dykes from the autochthonous basement east of the present Caledonian erosional margin (Fig. 1). According to the diagram of Winchester & Floyd (1977), these dykes comprise dominantly subalkaline basalts (Fig. 15). Two samples (G84:36, G96-16A-1) with relatively high Nb contents plot, however, beyond the line Nb/Y = 0.67. The sample G84:36 has increased K_2O, Rb, Ba and Sr, which indicates modification of original composition possibly due to assimilation of crustal material (Table 1). The sample G96-16A-1 has increased Na_2O contents, which may also indicate assimilation of crustal material and modification of primary composition. SiO_2 contents vary from 41.4 to 54.2 %, K_2O contents from 0.6 to 2.5 %, Na_2O contents from 1.3 to 4.3 %, TiO_2 contents from 0.67 to 3.75 %, and MgO contents from 3.08 to 11.62 % with Mg no. varying from 20 to 52.3. The TiO_2 contents show a bimodal distribution: a low-TiO_2 suite with TiO_2 contents varying from 0.7 to 1.9 % (average 1.4 %) and a high-TiO_2 suite with TiO_2 contents varying from 2.7 to 3.8 % (average 3.4 %). High-TiO_2 dykes are dominantly distributed in the Storuman–Stensele

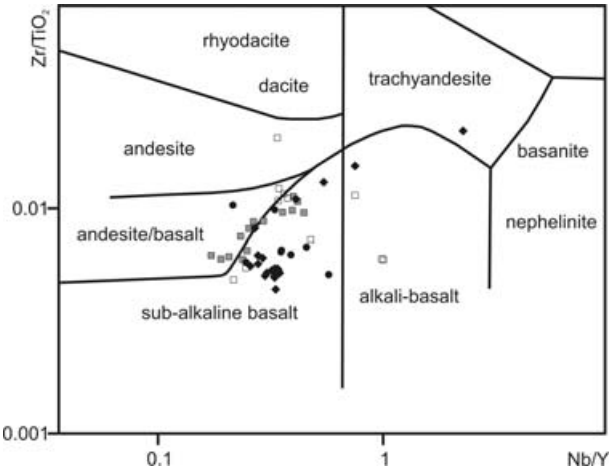

Figure 15. The classification diagram of Winchester & Floyd (1977) shows sub-alkaline basalts and andesites as the dominant dyke lithologies. Legend is the same as in Figures 12 and 13. For comparison, the Särv-type dykes (dots) are added.

area. Low-TiO_2 dykes are found preferentially in the Lycksele and Dorotea areas. Both low- and high-TiO_2 dykes are present in Vilhelmina area. TiO_2 contents are inversely correlated with Cr contents: high-TiO_2 dykes show low Cr contents and low-TiO_2 dykes have high Cr contents, comparable to Cr contents in MORB (Table 1, Fig. 16). The MORB-normalized spider diagram shows an enrichment of mobile and incompatible elements (Fig. 16) with a negative Nb-anomaly. This pattern is in agreement with continental tholeiites derived from an enriched continental lithospheric mantle source (e.g. Wilson, 1989).

https://doi.org/10.1017/S0016756807003299 Published online by Cambridge University Press

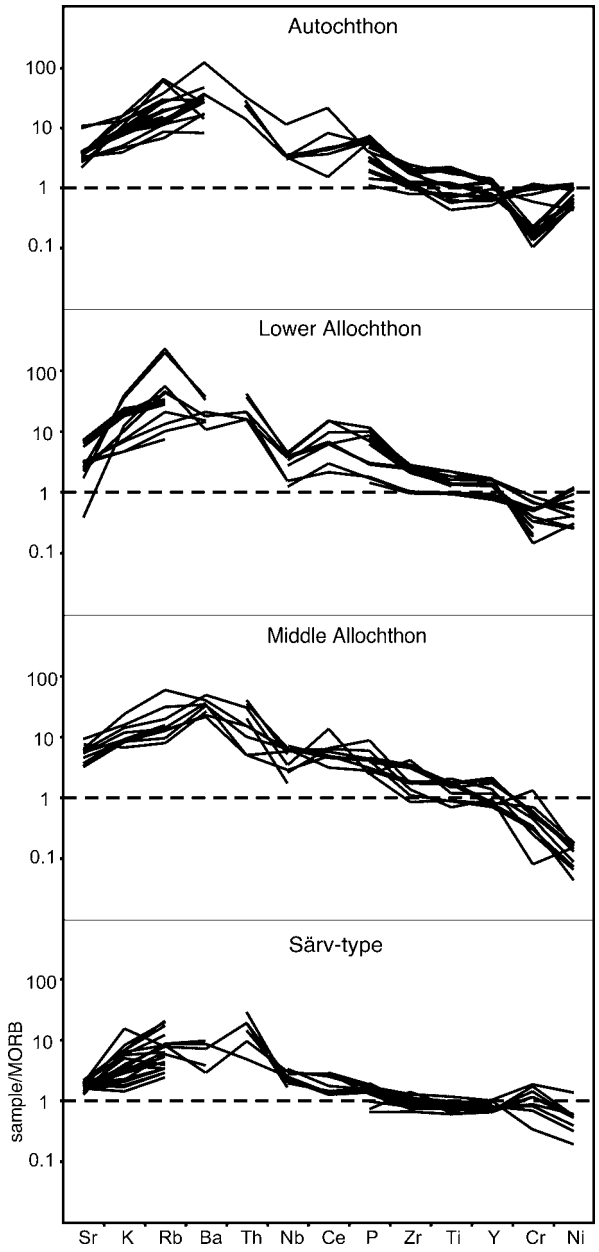

Figure 16. Multi-element, MORB-normalized (spider) diagrams from the dykes in the Autochthon, the Lower and Middle allochthons, and Särv-type dykes. Normalization values for MORB are adopted from Pearce (1983). The value for Cr is from Pearce (1982).

5.b. Lower Allochthon dykes

The analysed 24 samples from eight locations are collected from dykes in crystalline basement rocks of the Lower Allochthon. According to the diagram of Winchester & Floyd (1977), these dykes comprise dominantly subalkaline basalts and andesitic basalts (Fig. 15). SiO_2 contents vary from 44.8 to 52.9 %, K_2O contents from 0.7 to 5.7 %, Na_2O contents from 2.0 to 4.6 %, TiO_2 contents from 1.3 to 3.1 %, and MgO contents from 4.0 to 9.7 % with Mg no. varying from 27.3 to 42.3. The MORB-normalized spider diagram shows an enrichment of mobile and incompatible elements (Fig. 16) with a negative Nb-anomaly. This pattern is similar to that of the autochthonous dykes and is thus also in agreement with continental tholeiites.

5.c. Middle Allochthon dykes

5.c.1. Dykes in lower units of the Middle Allochthon

The analysed 11 samples from eight locations were collected from dykes which intruded basement rocks of the Middle Allochthon. According to the diagram of Winchester & Floyd (1977), these dykes comprise dominantly subalkaline and andesitic basalts (Fig. 15). Three samples (G84:2, MG84:02, MG84:04) plot, however, beyond the line $Nb/Y = 0.67$. G84:2 has relatively high Na_2O and K_2O contents, which indicates assimilation of crustal material possibly obtained during shearing. The samples MG84:02 and MG84:04 have relatively high Cr and Ni contents and high Mg no., indicating low degrees of fractionation. Assimilation of crustal material probably modified these relatively primitive melts. SiO_2 contents vary from 42.0 to 53.2 %, K_2O contents from 1.0 to 3.6 %, Na_2O contents from 1.3 to 5.2 %, TiO_2 contents from 1.0 to 3.1 % and MgO contents from 3.3 to 10.0 % with Mg no. varying from 24.3 to 42.3. The MORB-normalized spider diagram also shows LILE-enrichment (Fig. 16) with a weak negative Nb-anomaly, which is, however, not present in all samples. In contrast to the Lower Allochthon and the Autochthon there is a marked Ni-depletion.

5.c.2. Dykes in Särv Nappe equivalents

The analysed 23 samples from 11 locations of the Särv unit display a compositionally relatively homogeneous group (Table 1, Figs 15, 16), which can be distinguished from the dykes of the other tectonic units. SiO_2 contents vary from 43.3 to 52 %, K_2O contents from 0.2 to 2.4 %, Na_2O contents from 1.7 to 3.2 %, TiO_2 contents from 0.9 to 1.8 %, and MgO contents from 5.6 to 10.9 % with Mg no. varying from 33 to 49.4. Compared with the other dykes, relatively high degrees of partial melting are implied by the rather flat patterns in the MORB-normalized spider diagram (Fig. 16), which corroborates the MORB magmatic signature for the compatible to moderately compatible elements as well. A very weak negative to absent Nb-anomaly may indicate less of a continental influence than in the other units and a magmatic signature in agreement with E-MORB (Fig. 16).

6. Discussion and conclusions

Dykes in the northern, Västerbotten complex of the Central Scandinavian Dolerite Group can be mapped comprehensively from the existing magnetic anomaly

https://doi.org/10.1017/S0016756807003299 Published online by Cambridge University Press

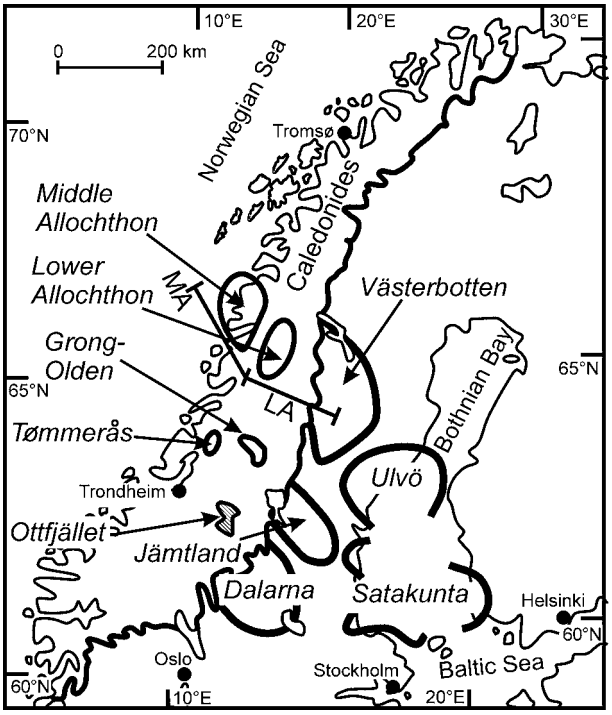

Figure 17. Outline of the western part of the Fennoscandian Shield with the dyke complexes that comprise the Central Scandinavian Dolerite Group as defined by Gorbatschev, Solyom & Johansson (1979) and modified by Hogmalm *et al.* (2006). Following Gayer & Greiling (1989), the areas of studied dykes in the Lower and Middle allochthons are restored along lines LA and MA, respectively. These areas show the probable pre-Caledonian extent of the mafic dyke swarms. In addition, the locations of dykes in the Lower Allochthon of the Grong-Olden and Tømmerås areas are indicated in their present, unrestored position, together with the Ottfjället area, as in Figure 1.

maps (Fig. 3) and show at least three different orientations, NW–SE, NE–SW and WNW–ESE, respectively. They are part of the autochthonous foreland of the Scandinavian Caledonides in the west (Figs 1, 17). Similar dykes are exposed in allochthonous positions in the Caledonian fold-and-thrust belt. Preliminary age information from a dyke in the Lower Allochthon of the Børgefjell area (Söderlund, pers. comm. 2006) and the Middle Allochthon (Greiling, Stephens & Persson, 2002) is consistent with the assumption that the dykes in these Caledonian allochthons are time equivalent with the Central Scandinavian Dolerite Group. According to section restorations, all of the Caledonian allochthons were situated further WNW relative to their present position (Gayer & Greiling, 1989). The restored, pre-Caledonian positions of the dykes in the Lower Allochthon and the Middle Allochthon (excluding the Särv Nappe) are shown schematically on Figure 17. Providing the preliminary age data can be confirmed, the areas marked Lower and Middle Allochthon, respectively, show an extension of the Västerbotten complex or a new complex of the Central Scandinavian Dolerite Group.

6.a. Fabric changes during progressive deformation and metamorphism, and rheology

6.a.1. Macroscopic and microstructural aspects

The autochthonous dykes are generally undeformed and retain both their primary texture and their primary mineralogy. Chilled margins are very well preserved. In the Caledonian Lower and Middle allochthons, similar dykes in crystalline basement rocks are progressively faulted and sheared when proceeding from the marginal to the interior parts of the orogen. In general, there is an increase in deformation intensity from the external to the internal units.

Dyke rock fabrics show a transition from brittle faulting to ductile shearing in the western, interior part of the Lower Allochthon. Dyke margins are more likely to be sheared than the interior parts of dykes. Apparently, minerals oriented favourably, that is, subparallel with shear surfaces, were most easily overprinted by shearing. In the Lower Allochthon, under very low- and low-grade metamorphic conditions, dykes are distinctly less competent than granitic host rocks. Dykes tens of metres thick are more competent than mica-rich gneisses, whereas decimetre-thick dykes do not show competence contrasts with such host-rock gneisses.

In the Middle Allochthon, dykes are generally sheared, although to varying degrees. While in low strain domains, metre-scale dykes with patches of altered plagioclase phenocrysts can still be discerned, highly sheared dykes are drawn out to thin layers of centimetre thickness. Dykes are deformed together with the crystalline country rocks under greenschist-grade metamorphic conditions without major competence contrasts. The microstructure generally indicates a predominance of simple shear deformation and a retrogression of the primary, high-temperature igneous mineral assemblage.

The Särv Nappes, which are transitional between the Middle and Upper allochthons, are dominated by quartzofeldspathic sedimentary rocks. There, structural studies by Gilotti & Kumpulainen (1986) showed the dykes to mechanically strengthen the rock units. Our observations indicate that the dykes are more competent than the metasedimentary country rocks. Microstructurally, the Särv-type dykes are distinct from the other dykes in the Lower and Middle allochthons in that they record a (prograde) thermal event after early deformation.

6.a.2. Magnetic fabrics

Magnetic fabrics show an evolution similar to the silicate mineral fabrics in general. However, due to progressive changes in magneto-mineralogy with progressive metamorphism, the magnetic character of the mafic dykes changes substantially. The magnetic fabrics are transformed successively from ferromagnetic–magmatic in the Fennoscandian Shield

https://doi.org/10.1017/S0016756807003299 Published online by Cambridge University Press

to ferromagnetic deformational in the Lower Allochthon and, finally, paramagnetic deformational in the Middle Allochthon. As a consequence of these changes, the magnetic susceptibility decreases for several orders of magnitude. Therefore, the dykes with the paramagnetic fabrics can no longer be distinguished as magnetic anomalies. The primary, ferromagnetic–magmatic fabric may represent a flow fabric, parallel with, for example, the WNW–ESE-trending dykes (Elming & Mattsson, 2001). It is important to note that this direction is parallel to a proposed palaeomagnetic direction (Elming & Mattsson, 2001). As discussed, for example, by de Wall & Greiling (2000), it is possible that the palaeomagnetic direction may be influenced by the AMS. Furthermore, the direction of the putative flow fabric is parallel with the linear fabric in the Caledonian thrust units (see Fig. 14c). Further work may be needed to establish whether there is a 'Caledonian' component in this fabric. Therefore, the distinction of different dyke generations based on different palaeomagnetic directions, as proposed by Elming & Mattsson (2001) and Elming, Moakhar & Martinsson (2004), may not be unequivocal.

6.b. Geochemistry

Geochemical analyses show a strong variation, which may be characteristic for dykes from the Central Scandinavian Dolerite Group (Söderlund *et al.* 2006). Dykes from the Dalarna Group of the Central Scandinavian Dolerite Group show a large scatter of ε_{Nd} values, which is indicative of crustal contamination (Patchett *et al.* 1994). Those samples, with $Nb/Y > 0.67$ may also indicate crustal contamination. However, it cannot be ruled out that samples with $Nb/Y < 0.67$ are free of crustal contamination. In the autochthonous dykes, different TiO_2 contents may indicate at least two different magma series: a high TiO_2 magma suite in the Vilhelmina and Storuman areas and a low TiO_2 magma suite in the Dorotea and Lycksele areas. There, the Orrkulla intrusion (sample suite G95:Ly; Table 1) has a precise $^{207}Pb/^{206}Pb$-baddeleyite age of 1259 ± 2.5 Ma (Söderlund *et al.* 2006). For comparison, the Särv-type dykes have a close range of relatively low TiO_2 contents, but variable Mg no. Ti contents indicate a relatively homogeneous mantle source; Mg numbers suggest various degrees of fractionation. The MORB-normalized multi-element spider diagrams of the Autochthon, Lower Allochthon and Middle Allochthon dykes show a strong enrichment of large ion lithophile elements (LILE) and other incompatible elements, which is in agreement with continental tholeiites.

Much debate has been focused on the interpretation of geochemical data concerning crustal contamination of basaltic rocks during ascent, storage and final emplacement in the crust (e.g. White & McKenzie, 1989; Arndt & Christensen, 1992; Peng *et al.* 1994; Patchett *et al.* 1994; Peate & Hawkesworth, 1996). The present data do not show obvious correlations between the intensity of metamorphic and deformational overprint and changes in the geochemical composition. Apparently, mineral changes did not lead to the transfer of elements across the dyke boundaries. Therefore, the geochemical enrichment of mobile and incompatible elements may be the primary feature of an enriched continental mantle lithosphere or, alternatively, it took place during early stages of ascent and thus reflects crustal contamination.

6.c. Tectonic and palaeogeographic implications

The Central Scandinavian Dolerite Group may have extended originally beyond the present Fennoscandian Shield, as already suggested by Solyom, Lindquist & Johansson (1992) and Elming & Mattsson (2001) with regard to a Greenland connection. The present Caledonian nappe sequence from bottom to top restores palaeogeographically to a sequence from ESE to WNW, with the Lower and Middle allochthons representing a continent–shelf transition and the Särv Nappe an outer shelf or continent–ocean transition. The distribution of the mafic dykes in the Caledonian nappes, as documented here, indicates a much wider westward extension than was known earlier (Johansson, 1980; Gorbatschev *et al.* 1987). The potential equivalents of the Central Scandinavian Dolerite Group appear to cut across all of the Fennoscandian lithosphere, until at least the present Atlantic margin and also to the earlier passive margin of the continental Baltica terrane. As a consequence, these dykes may provide a link for pre-Caledonian and pre-Grenvillian plate reconstructions.

Acknowledgements. The present paper is a result of the cooperation between the Geological Survey of Sweden, Uppsala, and Geologisch-Paläontologisches Institut of the Ruprecht-Karls-University, Heidelberg. We thank these institutions for their support, and G. Froelich, E. Hofmann, R. Koch and L. Nano for assistance with computing. Constructive reviews and comments by K. Obst (Greifswald), U. Söderlund (Lund), and suggestions for improvement by J. Holland (Cambridge) are gratefully acknowledged.

References

ANDRÉASSON, P.-G. 1994. The Baltoscandian Margin in Neoproterozoic – early Palaeozoic times. Some constraints on terrane derivation and accretion in the Arctic Scandinavian Caledonides. *Tectonophysics* **231**, 1–32.

ARNDT, N. T. & CHRISTENSEN, U. 1992. The role of lithospheric mantle in continental flood volcanism: thermal and geochemical constraints. *Journal of Geophysical Research* **97**, 10967–81.

BJÖRK, L. & KERO, L. 2002. *Bedrock maps 22I Lycksele, scale 1:50000*. Sveriges Geologiska Undersökning Series Ai no. 164–7.

BJÖRK, L., KERO, L. & ZACHRISSON, E. 2000. *Bedrock map Vilhelmina SO, scale 1:50000*. Sveriges Geologiska Undersökning Series Ai no. 87.

https://doi.org/10.1017/S0016756807003299 Published online by Cambridge University Press

CLAESSON, S. & RODDICK, J. C. 1983. $^{40}Ar/^{39}Ar$ data on the age and metamorphism of the Ottfjället dolerites, Särv Nappe, Swedish Caledonides. *Lithos* **16**, 61–73.

CONDIE, K. C. 2003. Supercontinents, superplumes and continental growth: the Neoproterozoic record. In *Proterozoic East Gondwana: Supercontinent Assembly and Breakup* (eds M. Yoshida, B. F. Windley & S. Dasgupta), pp. 1–21. Geological Society of London, Special Publication no. 206.

DE WALL, H. & GREILING, R. O. 2000. Remagnetisation and magnetic refraction in Proterozoic dykes from Central Scandinavia during Caledonian deformation. *Physics and Chemistry of the Earth* **A 25**, 519–24.

ELMING, S.-Å. & MATTSSON, H. J. 2001. Post Jotnian basic intrusions in the Fennoscandian Shield, and the break-up of Baltica from Laurentia: a palaeomagnetic and AMS study. *Precambrian Research* **108**, 215–36.

ELMING, S.-Å., MOAKHAR, M. O. & MARTINSSON, O. 2004. A palaeomagnetic and geochemical study of basic intrusions in northern Sweden. *Geologiska Föreningens Stockholm Förhandlingar* **126**, 243–52.

ERNST, R. E. & BUCHAN, K. L. 2001*a*. The use of mafic dike swarms in identifying and locating mantle plumes. *Geological Society of America Special Paper* **352**, 247–65.

ERNST, R. E. & BUCHAN, K. L. 2001*b*. Large mafic magmatic evens through time and links to mantle-plume heads. *Geological Society of America Special Paper* **352**, 483–575.

FOSLIE, S. & STRAND, T. 1956. Namsvatnet med en del av Frøyningsfjell. *Norges Geologiske Undersökelse* **196**, 1–82.

GAYER, R. A. & GREILING, R. O. 1989. Caledonian nappe geometry in north-central Sweden and basin evolution on the Baltoscandian margin. *Geological Magazine* **126**, 499–513.

GEE, D. G. & KUMPULAINEN, R. 1980. An excursion through the Caledonian mountain chain in central Sweden from Östersund to Storlien. *Sveriges Geologiska Undersökning Series C* **774**, 66 pp.

GEE, D. G. & ZACHRISSON, E. 1973. The Caledonides in Sweden. *Sveriges Geologiska Undersökning Series C* **769**, 48 pp.

GILOTTI, J. & KUMPULAINEN, R. 1986. Strain softening induced ductile flow in the Särv thrust sheet, Scandinavian Caledonides. *Journal of Structural Geology* **8**, 441–55.

GORBATSCHEV, R., LINDH, A., SOLYOM, Z., LAITAKARI, I., ARO, K., LOBACH-ZHUCHENKO, S. B., MARKOV, M. S., IVLIEV, A. I. & BRYHNI, I. 1987. Mafic Dyke Swarms of the Baltic Shield. *Geological Association of Canada, Special Paper* **34**, 361–72.

GORBATSCHEV, R., SOLYOM, Z. & JOHANSSON, I. 1979. The Central Scandinavian Dolerite Group in Jämtland, central Sweden. *Geologiska Föreningen Stockholm Förhandlinga* **101**, 177–90.

GREILING, R. O. 1982. Precambrian basement complexes in the north-central Scandinavian Caledonides and their Caledonian tectonic evolution. *Geologische Rundschau* **71**, 85–93.

GREILING, R. O. 1985. Strukturelle und metamorphe Entwicklung an der Basis grosser, weittransportierter Deckeneinheiten am Beispiel des Mittleren Allochthons in den zentralen Skandinavischen Kaledoniden (Stalon-Deckenkomplex in Västerbotten, Schweden). *Geotektonische Forschungen* **69**, 129 pp.

GREILING, R. O. 1988. *Ranseren, berggrunnskart 2025/3, 1:50000, foreløpig utgave*. Norges Geologiske Undersökelse.

GREILING, R. O., GARFUNKEL, Z. & ZACHRISSON, E. 1998. The orogenic wedge in the central Scandinavian Caledonides: Scandian structural evolution and possible influence on the foreland basin. *Geologiska Föreningens Stockholm Förhandlingar* **120**, 181–90.

GREILING, R. O., GAYER, R. A. & STEPHENS, M. B. 1993. A basement culmination in the Scandinavian Caledonides formed by antiformal stacking (Bångonåive, northern Sweden). *Geological Magazine* **130**, 471–82.

GREILING, R. O., GORBATSCHEV, R., JOHANSSON, L. & EBERZ, G. 1984. Chemical variation and tectonic significance of some Middle and Late Proterozoic dyke swarms in the central Scandinavian Caledonides and their foreland. *Terra Cognita* **4**, 88–9.

GREILING, R. O., STEPHENS, M. B. & PERSSON, P.-O. 2002. Crystalline basement rocks in the Lower and Middle Allochthons, Västerbotten, Sweden: Palaeoproterozoic U–Pb zircon ages from the north-central Swedish Caledonides. *Sveriges Geologiska Undersökning Series C* **834**, 31–42.

GREILING, R. O. & ZACHRISSON, E. 1999. *Berggrundskartan 23 G Dikanäs NV, SV scale 1:50000*. Sveriges Geologiska Undersökning Serie Ai, nos 122, 123.

GREILING, R. O., ZACHRISSON, E., BJÖRK, L. & KERO, L. 1996. *Berggrundskartan 22 G, Vilhelmina NO, scale 1:50000.* Sveriges Geologiska Undersökning Serie Ai no. 86.

GUSTAVSON, M. 1973. *Børgefjell. Beskrivelse til det berggrunnsgeologiske gradteigskart J.19 1:100000*. Norges Geologiske Undersökelse, vol. 298, 43 pp.

HARGRAVES, R. B., JOHNSON, D. & CHAN, C. Y. 1991. Distribution anisotropy: the cause of AMS in igneous rocks? *Geophysical Research Letters* **18**, 2193–6.

HELLSTRÖM, F. A. & LARSON, S. Å. 2003. U–Pb zircon dating of the Hoting gabbro, north central Sweden. *Geologiska Föreningens Stockholm Förhandlingar* **125**, 221–8.

HÖGDAHL, K., ANDERSSON, U. B. & EKLUND, O. 2004. The Transscandinavian Igneous Belt in Sweden: a review of its character and evolution. *Geological Survey of Finland, Special Paper* **37**, 125 pp.

HOGMALM, K. J., SÖDERLUND, U., LARSON, S. Å., MEURER, W. P., HELLSTRÖM, F. A. & CLAESON, D. T. 2006. The Ulvö Gabbro Complex of the 1.27–1.25 Ga Central Scandinavian Dolerite Group (CSDG): Intrusive age, magmatic setting and metamorphic history. *Geologiska Föreningen Stockholm Förhandlinga* **128**, 1–6.

JELINEK, V. 1981. Characterization of the magnetic fabrics of rocks. *Tectonophysics* **79**, 63–7.

JOHANSSON, L. 1980. Petrochemistry and regional tectonic significance of metabasites in basement windows of the central Scandinavian Caledonides. *Geologiska Föreningens i Stockholm Förhandlingar* **102**, 499–514.

KATHOL, B. & WEIHED, P. 2005. Description of regional geological and geophysical maps of the Skellefte District and surrounding areas. *Sveriges Geologiska Undersökning Serie Ba* **57**, 197 pp.

KNIGHT, M. D. & WALKER, G. P. L. 1988. Magma flow directions in dykes of the Koolau Complex, Oahu, determined from magnetic fabric studies. *Journal of Geophysical Research* **93**, 4301–19.

KOISTINEN, T., STEPHENS, M. B., BOGATCHEV, V., NORDGULEN, Ø., WENNERSTRÖM, M. & KORHONEN, J. 2001.

Geological map of the Fennoscandian Shield, scale 1:2000000. Geological Surveys of Finland, Norway and Sweden and the North–West Department of Natural Resources of Russia.

KONTNY, A. & DE WALL, H. 2000. Case studies on the use of temperature-dependent susceptibility for the characterization of magneto-mineralogical changes during metamorphism. *Physics and Chemistry of the Earth* **A25**, 421–9.

LUNDQVIST, T. & AUTIO, S. 2000. Description to the Bedrock Map of Central Fennoscandia (Mid-Norden). *Geological Survey of Finland, Special Paper* **28**, 176 pp.

PATCHETT, P. J., LEHNERT, K., REHKÄMPER, M. & SIEBER, G. 1994. Mantle and Crustal Effects on the Geochemistry of Proterozoic Dikes and Sills in Sweden. *Journal of Petrology* **35**, 1095–1125.

PEARCE, J. A. 1982. Trace element characteristics of lavas from destructive plate boundaries. In *Andesites* (ed. R. S. Thorpe), pp. 525–48. Chichester: Wiley.

PEARCE, J. A. 1983. Role of the sub-continental lithosphere in magma genesis at active continental margins. In *Continental basalts and mantle xenoliths* (eds C. J. Hawkesworth & M. J. Norry), pp. 230–49. Nantwich: Shiva.

PEATE, D. W. & HAWKESWORTH, C. J. 1996. Lithospheric to asthenospheric transition in low-Ti flood basalts from southern Parana. *Brazilian Chemical Geology* **127**, 1–24.

PENG, Z. X., MAHONEY, J. J., HOOPER, P., HARRIS, C. & BEANE, J. 1994. A role for lower continental crust in flood basalt genesis? Isotopic and incompatible element study of the lower six formations of the western Deccan Traps. *Geochimica et Cosmochimica Acta* **58**, 267–88.

ROCHETTE, P., JACKSON, M. & AUBOURG, C. 1991. Rock magnetism and the interpretation of anisotropy of magnetic susceptibility. *Reviews of Geophysics* **30**, 209–26.

SÖDERLUND, U., ELMING, S.-Å., ERNST, R. E. & SCHISSEL, D. 2006. The Central Scandinavian Dolerite Group – protracted hotspot activity or back-arc magmatism? Constraints from U–Pb baddeleyite geochronology and Hf isotopic data. *Precambrian Research* **150**, 136–52.

SÖDERLUND, U., ISACHSEN, C. E., BYLUND, G., HEAMAN, L. M., PATCHETT, P. J., VERVOORT, J. D. & ANDERSSON, U. B. 2005. U–Pb baddeleyite ages and Hf, Nd isotope chemistry constraining repeated mafic magmatism in the Fennoscandian Shield from 1.6 to 0.9 Ga. *Contributions to Mineralogy and Petrology* **150**, 174–94.

SOLYOM, Z., GORBATSCHEV, R. & JOHANSSON, I. 1979. The Ottfjäll Dolerites: geochemistry of the dyke swarm in relation to the geodynamics of the Caledonide orogen of Central Scandinavia. *Sveriges Geologiska Undersökning Series C* **756**, 35 pp.

SOLYOM, Z., LINDQUIST, J.-E. & JOHANSSON, I. 1992. The geochemistry, genesis, and geotectonic setting of Proterozoic mafic dyke swarms in southern and central Sweden. *Geologiska Föreningens Stockholm Förhandlingar* **114**, 47–65.

STÅLHÖS, G. 1958. En bäddforming jotnisk diabas i norra Västerbotten. *Geologiska Föreningen Stockholm Förhandlingar* **80**, 55–8.

STEPHENS, M. B., WAHLGREN, C.-H. & WEIHED, P. 1997. Sweden. In *Encyclopedia of European and Asian regional geology* (eds E. M. Moores & R. W. Fairbridge), pp. 690–704. London: Chapman & Hall.

STEPHENSON, A. 1994. Distribution anisotropy: two simple models for magnetic lineation and foliation. *Physics of the Earth and Planetary Interiors* **82**, 49–53.

TARLING, D. H. & HROUDA, F. 1993. *The Magnetic Anisotropy of Rocks*. London: Chapman & Hall, 217 pp.

TARNEY, J. 1992. Geochemistry and significance of Mafic Dyke swarms in the Proterozoic. In *Proterozoic Crustal Evolution* (ed. K. C. Condie), pp. 151–77. Amsterdam, New York, Tokyo: Elsevier.

WHITE, R. S. & MCKENZIE, D. P. 1989. Magmatism at rift zones: the generation of volcanic continental margins and flood basalts. *Journal of Geophysical Research* **94**, 7685–730.

WILSON, M. 1989. *Igneous Petrogenesis – a Global Tectonic Approach*. London: Chapman & Hall, 466 pp.

WINCHESTER, J. A. & FLOYD, P. A. 1977. Geochemical discrimination of different magma series and their differentiation products using immobile elements. *Chemical Geology* **20**, 325–43.

WINDLEY, B. F. 2003. Continental growth in the Proterozoic: a global perspective. In *Proterozoic East Gondwana: Supercontinent Assembly and Breakup* (eds M. Yoshida, B. F. Windley & S. Dasgupta), pp. 23–33. Geological Society of London, Special Publication no. 206.

ZACHRISSON, E. 1991. *Bedrock maps 23E Sipmeke, scale 1:50000*. Sveriges Geologiska Undersökning Series Ai no. 73–4.

ZACHRISSON, E. & GREILING, R. O. 1993. *Bedrock maps 23F Fatmomakke NO, SO, 1:50000*. Sveriges Geologiska Undersökning Series Ai no. 77–8.

ZACHRISSON, E. & GREILING, R. O. 1996. *Bedrock map 22 G Vilhelmina NV, 1:50000*. Sveriges Geologiska Undersökning Series Ai no. 84.